Innate immune signaling in trophoblast and decidua organoids defines differential antiviral defenses at the maternal-fetal interface

Liheng Yang[1], Christina Megli[2,3], Carolyn B. Coyne[1*]

[1]Department of Molecular Genetics and Microbiology, Duke University School of Medicine, Durham, NC USA, [2]Division of Maternal-Fetal Medicine, Division of Reproductive Infectious Disease, Department of Obstetrics, Gynecology and Reproductive Sciences, University of Pittsburgh Medical Center (UPMC),[3]Magee Womens Research Institute, Pittsburgh, PA USA

*Address correspondence
Carolyn Coyne, PhD
3130 Medical Sciences Research Building III
3 Genome Court
Durham, NC 27710
USA
carolyn.coyne@duke.edu

Abstract

Infections at the maternal-fetal interface can directly harm the fetus and induce additional complications that adversely impact pregnancy outcomes. Innate immune signaling by both fetal-derived placental trophoblasts and the maternal decidua must provide antimicrobial defenses at this critical interface without compromising its integrity. Here, we developed matched trophoblast and decidua organoids from human placentas to define their relative contributions to innate immune antiviral defenses at the maternal-fetal interface. We show that trophoblast and decidua organoids recapitulate some, but not all, of the basal cytokine release observed in matched tissue explants. We further show that trophoblast organoids constitutively release antiviral type III interferons (IFNs) and that fetal and maternal organoids differentially respond to viral infections through the induction of organoid-specific cytokines. These findings define key differences in innate immune signaling generated by fetal-derived trophoblasts and the maternal decidua, which together must protect the fetus from viral infections.

Introduction

The maternal-fetal interface is comprised of both the maternal-derived decidua and the fetal-derived placenta, which together support fetal growth and provide immunologic defenses that protect the fetus from infections. The relative contributions of specific maternal- and fetal-derived cells to these critical functions remain largely undefined given the limitations of models that recapitulate the complex nature of this interface.

The placenta forms a key barrier to viral vertical transmission throughout pregnancy and is comprised in part by fetal-derived trophoblast cells. Trophoblast stem cells located in chorionic villi, the branch like projections that directly contact maternal blood, give rise to cytotrophoblasts (CTBs), the proliferative mononuclear cells of the placenta, extravillous trophoblasts (EVTs), and the syncytiotrophoblast (STB), a multinucleated contiguous cell layer that covers the villous surfaces. EVTs directly remodel the maternal microvasculature to form spiral arteries, which ultimately deliver maternal blood to the surfaces of chorionic villi. Decidualization of the endometrium is required for implantation and appropriate placentation. This process involves the differentiation of fibroblast-like mesenchymal cells into secretory decidua cells. Prior to the formation of chorionic villi and the development of a hemochorial placenta, these secretory cells provide necessary nutrients to the developing embryo [1]. Together, the decidua and placenta thus provide the fetus with essential hormones and nutrients to support its growth.

While the placenta and decidua play complementary roles in fetal development, their contributions to antimicrobial defenses are less defined. Studies of tissue explants and histopathologic analysis of the placenta suggest that the decidua and chorionic villi have differing roles in the pathogenesis of relevant infections. The decidua may be a primary site of replication for several microorganisms associated with congenital disease, including cytomegalovirus (CMV) [2-4], Zika virus (ZIKV) [5-7], and *Listeria monocytogenes* [8], suggesting it may serve as a reservoir for these infections. By contrast, the placenta is largely resistant to infections and possesses several intrinsic mechanisms of innate defense. In the case of viruses, human trophoblasts constitutively

53 release antiviral interferons (IFNs) that restrict infection in both autocrine and paracrine manners [9,
54 10]. These IFNs are of the type III class, which include IFNs-λ1-3 in humans [11, 12]. Constitutive
55 release of IFNs is a unique feature of trophoblasts as IFNs are tightly regulated in most cell types
56 and induced only after detection of the products of viral replication. In mice, type III IFNs also confer
57 protection from Zika virus (ZIKV) vertical transmission and fetal disease, which occurs in a
58 gestational-associated manner [13, 14], although it is not clear whether mice constitutively release
59 these IFNs. Together, these findings suggest that maternal- and fetal-derived tissue differentially
60 respond to and control viral infections. However, the lack of available models to fully interrogate the
61 differences between maternal- and fetal-derived cells has limited a complete understanding of these
62 processes, including how each tissue type responds to infection.

63 The recent development of trophoblast and decidua organoids from first trimester placental
64 tissue has expanded the models available to study the maternal-fetal interface [15, 16]. Previous
65 work has shown that isolation and propagation of trophoblast stem cells from first trimester placental
66 chorionic villi leads to the development of three-dimensional organoids that differentiate to contain
67 all lineages of trophoblast cells present in the human placenta and release well-known pregnancy
68 hormones such as human chorionic gonadotropin (hCG) [15]. Similarly, decidua organoids isolated
69 from uterine glands recapitulate the transcriptional profile of their tissue of origin and respond to
70 hormonal cues [16]. These organoid models thus provide ideal systems to profile differences
71 between maternal- and fetal-derived cells, however, these models have not yet been applied to
72 pathogen infections.

73 To directly compare antiviral signaling pathways between the human placenta and decidua,
74 we generated trophoblast and decidual organoids from matched human placentas and profiled the
75 release of cytokines, chemokines, and other factors from these models under uninfected and virally
76 infected conditions. In parallel, we performed similar profiling in matched tissue explants from which
77 these organoids were developed and found that organoids produced distinct patterns of released
78 cytokines. To determine whether there are differences in the responses of maternal- and fetal-

79 derived cells to viral infections, we also compared the immunological secretome from organoids
80 treated with a ligand to stimulate toll-like receptor 3 (TLR3) signaling or after infection with ZIKV.
81 These studies revealed that trophoblast organoids selectively secrete the type III IFN IFN-λ2, which
82 does not occur in matched decidua organoids. Moreover, trophoblast and decidua organoids
83 differentially respond to TLR3 activation and ZIKV infection through the secretion of organoid-specific
84 cytokines. Our studies highlight the differential responses of key cells comprising the maternal-fetal
85 interface and provide new models to define the impact of pathogen exposure at this key site.
86

87 **Results**

88 **Establishment and characterization of human trophoblast and decidual organoids**

89 To generate matched human trophoblast organoids (TOs) and decidual organoids (DOs), we used
90 human placental tissue isolated from the second and third trimesters of human pregnancy and
91 cultured stem cells isolated from chorionic villi or isolated decidua in growth factor-containing medium
92 like that described previously [15-20] (**Figure 1A**). Although the abundance of villous stem cells
93 decreases after the first trimester [15], we successfully recovered organoids from all placental tissue
94 harvested (five unique placentas). Isolated stem cells were embedded in Matrigel to allow for self-
95 organization and propagated for ~3 weeks to generate organoid structures that were morphologically
96 similar to those described previously that were isolated from the first trimester [15, 16] (**Figure 1B**).
97 Also, like those isolated from the first trimester [15], cultured TOs developed projections that
98 resembled villous structures (**Figure 1B**, arrows at bottom). Confocal microscopy confirmed the
99 three-dimensional architecture of established organoids and verified that TOs expressed markers
100 such as cytokeratin-19 (**Figure 1C**) and DOs expressed markers including cytokeratin-7 and -19 and
101 E-cadherin (**Figure 1D**), consistent with previous reports [15, 16]. We also confirmed that TOs, but
102 not DOs, secreted the trophoblast-specific hormone human chorionic gonadotropin (hCG) by both
103 ELISA and rapid test strip assays (**Figure 1E**) and pregnancy-specific beta-1 glycoprotein 1 (PSG1)
104 by ELISA, a major product released from the STB, similar to chorionic villous explants (**Figure 1F**).

105 TOs could be propagated for at least three months and passaged approximately every 2 weeks with
106 stable hCG release (**Supplemental Figure 1A, 1B**).

107 Next, we performed transcriptional profiling of isolated TOs and DOs using RNASeq. We
108 found that TOs and DOs were transcriptionally distinct based on volcano and principal component
109 analysis (PCA) plots (**Figure 2A**, **Supplemental Figure 2A, 2B**). TOs highly expressed transcripts
110 specifically enriched in the placenta, including HSD3B1, XAGE2 and 3, GATA3, and ERVW-1, which
111 were absent or expressed at very low levels in DOs (**Figure 2B**). In addition, TOs highly expressed
112 transcripts for PSGs and hCG (**Figure 2B**). The levels of expression of these transcripts were
113 equivalent to those in primary human trophoblasts, confirming that TOs recapitulate the
114 transcriptional signature of primary cells (**Figure 2B**). These markers were consistent with the
115 presence of the syncytiotrophoblast (e.g., CGA, PSGs, CSH1, HSD3B1), cytotrophoblasts (e.g.,
116 TP63, ITGA6), and extravillous trophoblasts (e.g., ITGA5, HLA-G) (**Figure 2B**). In contrast, DOs
117 expressed markers associated with the decidua and decidual stromal cells, including MUC1, MUC5A,
118 MUC5B, and SOX17, which were absent or expressed at low levels in TOs and PHT cells (**Figure**
119 **2B**). To further confirm that TOs and DOs recapitulated their tissues of origin, we profiled the
120 expression of three members of the chromosome 19 microRNA family (C19MC), which are
121 specifically expressed in the human placenta [21]. We found that miR-516B-5p, miR-517A-3p, and
122 miR-525-5p were expressed at high levels in TOs, comparable to levels observed in freshly isolated
123 chorionic villi, but were not expressed in DOs (**Figure 2C**). Lastly, we found that TOs isolated from
124 placentas obtained from male fetuses expressed Y-linked genes, which were absent in female-only
125 derived DOs (**Supplemental Figure 2C**). Collectively, these data establish matched TOs and DOs
126 as model systems of the maternal-fetal interface and that they can be isolated from tissue after the
127 first trimester, including from mid-to-late in gestation.

128

129 **Cytokine profiling of TOs and DOs compared to matched tissue explants**

130 We have shown previously that human chorionic villous explants release a number of cytokines,
131 chemokines, and growth factors that impact both maternal and fetal antimicrobial defenses [22].
132 Similarly, we have shown that primary human trophoblasts (PHTs) isolated from mid-gestation and
133 full-term placentas secrete some of these same immunoactive factors [10, 22]. We therefore profiled
134 the immunological secretome of TOs isolated from three independent placentas and compared these
135 profiles to chorionic villous explants isolated from the same placentas. In addition, we compared
136 these profiles to PHT cells to determine whether there were differences between stem cell-derived
137 trophoblasts and primary trophoblasts isolated directly from full-term tissue. To do this, we used
138 multianalyte Luminex-based profiling for ~80 cytokines, chemokines, growth and other factors from
139 conditioned media (CM) isolated from these models under unstimulated conditions. Factors whose
140 secretion was reliably measured over 50pg/mL were identified as present. We found that TOs
141 secreted two cytokines (IL-6 and IL-28A/IFN-λ2) and three immune-regulated secreted soluble
142 receptors (sTNF-R1, gp130/sIL-6Rβ, sTNF-R2) (**Figure 2A**). By contrast, matched chorionic villous
143 explants were immunologically more active and we reliably detected 51 factors (**Figure 2B**). Similarly,
144 PHT cells also released a greater number of factors, with 31 detected (**Figure 2C**). The five factors
145 released from TOs were also released from chorionic villous explants and PHT cells (**Figure 2D**).
146 The most abundant cytokine present in CM isolated from TOs was IL-6, which was released at levels
147 similar to those observed in both chorionic villi and PHT cells (**Figure 2E**). In contrast, whereas the
148 most abundant factor in CM isolated from PHT cells was IL-8, which was also highly abundant in CM
149 from chorionic villi, this cytokine was not detected in CM isolated from TOs, suggesting that there
150 might be differential immune regulation between terminally differentiated PHT cells and those that
151 are stem-cell derived (**Figure 2F**).

152 To define the immunological secretome of DOs, we performed similar Luminex-based
153 profiling as the studies described above from CM isolated from DOs and decidua explants.
154 Compared to TOs, DOs released a larger number of factors overall, with 21 detected in DO-derived
155 CM (**Figure 3A**). Of these, 19 were also released from human decidua explants, which contained

156 50 total cytokines and other factors (**Figure 3B, 3C**). DOs and decidua explant tissue secreted similar
157 levels of factors such as MMP-1 (**Figure 3D**). In contrast, we found that DOs secreted high levels of
158 IL-10, which was not detected in CM from decidua explants (**Figure 3E**). Together, these data
159 suggest that TOs and DOs partially recapitulate the secretion profile of chorionic villi and the decidua.
160

161 **Trophoblast organoids constitutively secrete antiviral IFN-λs**

162 We next directly compared the secretion profiles from CM collected from matched TOs and DOs to
163 identify factors enriched in either maternal- or fetal-derived cells. TOs selectively secreted two
164 cytokines that were not present in CM isolated from matched DOs, IL-6 and IFN-λ2 (**Figure 4A-B,**
165 **D).** In contrast, DOs selectively released high levels of other factors such as IL-8 (**Figure 4C**). We
166 showed previously that PHT cells isolated from full-term placentas and mid-gestation chorionic villi
167 constitutively release type III IFNs, which protect from viral infections [9, 10]. We found that TOs
168 recapitulated this phenotype and released high levels of IFN-λ2, but not type I IFNs or IFN-λ1 (**Figure**
169 **4E**). In contrast, DOs did not basally secrete any detectable IFNs (**Figure 2A, 4D**). Consistent with
170 this, the expression of type III IFN transcripts was very high in TOs, but not DOs (**Figure 3F**). We
171 monitored the release of IFN-λ2 over the growth period of TOs and found that it's release was
172 detectable by ~10-days post-plating and reached high levels by >14-days in culture, which correlated
173 with similar trends for IL-6 (**Supplemental Figure 3A**). We confirmed that CM isolated from TOs,
174 but not DOs, induced interferon stimulated genes (ISGs) using a HEK293 based reporter assay
175 (**Figure 4G**). Consistent with this, we found that CM isolated from TOs was antiviral and reduced
176 ZIKV infections in non-placental cells treated with this CM (**Figure 4H**). PHT cells basally express
177 high levels of ISGs, most likely from the autocrine effects of released IFN-λs [10]. Therefore, we
178 compared the basal expression of several ISGs in TOs and DOs and compared these levels to those
179 in PHT cells, and in two choriocarcinoma cell lines, JEG-3 and JAR cells, which do not basally
180 release type III IFNs [9]. We found that similar to PHT cells, TOs basally express high levels of ISGs,

181 which was not observed in either JEG-3 or JAR cells (**Supplemental Figure 3B**). However, despite
182 the absence of released IFN-λs, DOs also expressed high levels of these ISGs (**Supplemental**
183 **Figure 3B**). These data show that TOs recapitulate the constitutive release of type III IFNs observed
184 in primary trophoblast cells and tissue and that these IFNs function in paracrine to restrict viral
185 infections.
186
187 **Differential response to IFNs in TOs and DOs**
188 Previous work has shown that chorionic villous and decidua explants respond to treatment with
189 recombinant IFNs, which protect from ZIKV infection [13], although villous explants appear to be less
190 responsive to type III compared to type I IFNs [23]. However, given that the tissue used in these
191 studies contains many different cell types, we investigated the sensitivity of TOs and DOs to
192 recombinant type I (IFN-β) or type III (IFN-λ) treatment. We found that DOs were highly responsive
193 to both type I and III IFN treatment and robustly induced ISGs including IFI44L and OASL (**Figure**
194 **6A, 6B**). These ISGs were similarly induced by IFN treatment of decidua explants (**Figure 6C**).
195 Although TOs did respond to both type I and III IFN treatment, the magnitude of these responses
196 were lower than those in DOs (**Figure 6A, 6B**), which were consistent with the responses of IFN-
197 treated chorionic villous explants (**Figure 6C, 6D**). These data suggest that there are differences in
198 the sensitivity of maternal-and fetal-derived cells to type I and III IFNs.
199
200 **Differential induction of antiviral signaling in TOs and DOs**
201 Because we observed differences in the constitutive release of IFN-λ2 from TOs and DOs, we next
202 determined how these organoids responded to viral infections. To do this, we used poly (I:C), a
203 synthetic ligand of TLR3 and measured differences in cytokine induction using Luminex-based
204 profiling. We found that both TOs and DOs robustly responded to poly I:C treatment, which
205 corresponded with the induction of ISGs in both models, although TOs induced higher transcript

206 levels of these ISGs (**Supplemental Figure 4A**). Cytokine profiling of CM isolated from poly I:C-
207 treated TOs and DOs showed that TOs induced 15 factors (>5-fold change from mock) and DOs
208 induced 14 factors (>5-fold change from mock) in response to TLR3 activation (**Figure 7A**). Of the
209 factors induced, 9 were shared between both TOs and DOs (**Figure 7B**), which included IFN-λ1,
210 which was the most induced cytokine in both organoids (**Figure 7C**) and IFN-λ2 (**Figure 7D**). Several
211 cytokines were differentially induced in TOs versus DOs, including IFN-γ, which was induced in DOs
212 but not TOs (**Supplemental Figure 4B)** and IL-8**,** which was induced in TOs but not DOs
213 (**Supplemental Figure 4C).** In addition, we found that whereas TOs induced the type I IFNs IFN-α2
214 and IFN-β in response to poly I:C, DOs induced no IFN-α2 and low levels of IFN-β (**Figure 7E, 7F).**
215 We next profiled the differential response to viral infections in TOs and DOs using ZIKV. We
216 found that both TOs and DOs supported low levels of ZIKV replication as assessed by focus-forming
217 unit (FFU) assays at 72hrs post-infection (p.i.) (**Figure 8A**). However, levels of ZIKV infection were
218 significantly lower than those observed in permissive JEG-3 cells (**Figure 8A**). To determine the
219 impact of this infection on the transcriptional profiles of TOs and DOs, we performed RNASeq.
220 Consistent with the low levels of infection observed by FFU assays, there were very low levels of
221 viral RNA present in infected organoids, as determined by FPKM values (**Figure 8B**). Also consistent
222 with low levels of viral replication, there were no significant changes in the transcriptional profile of
223 ZIKV infected DOs (**Figure 8C**) and only changes in three transcripts in TOs (**Figure 8D**).
224 To determine if these transcriptional profiles were associated with changes in cytokine
225 release, we performed luminex-based profiling of CM isolated from these cultures at 24hrs, 48hrs,
226 and 72hrs p.i..This profiling showed that few cytokines were induced by ZIKV infection and no
227 cytokines or other factors were induced >5-fold in either TOs or DOs (**Figure 8E, 8F**). Consistent
228 with poly I:C treatment, TOs induced very low levels of IFN-λ1 and IFN-β at 72hrs p.i., which was
229 not observed in DOs (**Figure 8G, 8H**). In contrast, DOs secreted low levels of the
230 glycophosphoprotein osteopontin at 24hrs p.i., which decreased over the course of infection (**Figure**

231 **8I**). Taken together, these data show that TOs and DOs differentially respond to viral infections
232 through the release of select cytokines and other factors.
233

234 **Discussion**

235 Our work presented here establishes fetal- and maternal-derived organoids as models of
236 innate immune signaling at the maternal-fetal interface. We show that TOs constitutively secrete two
237 cytokines at high levels, the pro-inflammatory cytokine IL-6 and the antiviral IFN-λ2. In contrast, we
238 show that DOs are immunologically more active under resting conditions and basally secrete several
239 cytokines not observed in TOs, but do not release IFNs under unstimulated conditions. In addition,
240 we show that TOs and DOs differentially respond to TLR3 activation and ZIKV infection and induce
241 organoid-specific cytokines in response to activation of antiviral innate immune signaling. Collectively,
242 our work suggests that cells that comprise the maternal-fetal interface defend from viral infections in
243 a cell-type specific manner and highlight the unique contributions of fetal-derived trophoblasts in
244 antiviral immunity.

245 The previous establishment of trophoblast and decidua-derived organoids has significantly
246 expanded the *in vitro* systems that can model the complexity of the maternal-fetal interface [15, 16].
247 These previous studies utilized tissue isolated from the first trimester of pregnancy (6-9 weeks
248 gestation for TOs and 8-12 weeks gestation for DOs) [15, 16], although another study successfully
249 established DOs from full-term tissue [20]. Here, we show that TOs can also be isolated from later
250 stages of gestation, including from full-term placental tissue. Moreover, we show that the growth
251 medium and conditions used to grow organoids from first trimester tissue can be extrapolated to
252 grow organoids from the second and third trimesters of pregnancy. Two-dimensional cultures of stem
253 cell-derived primary trophoblasts are also restricted to tissue obtained in the first trimester [18]. Given
254 that access to first trimester tissue can be complicated by access and/or regulatory restrictions, our
255 studies provide an additional source for the development of placental organoids from tissue obtained

256 later in gestation. Moreover, the establishment of these organoids from tissues later in gestation may
257 allow for elucidation of the role of maternal-fetal signaling in obstetric related pathologies.

258 Unlike many other barrier cell types such as the epithelium, human trophoblasts have the
259 unique capacity to robustly secrete cytokines and other immunological factors without stimulation.
260 Primary human trophoblasts from full-term placentas and mid-gestation chorionic villi secrete
261 cytokines that mediate innate defenses from bacteria, parasites, and viruses [9, 22, 24]. Consistent
262 with this, serum isolated from pregnant women often contains elevated levels of these cytokines,
263 indicating that at least some have reached the systemic circulation [22, 25-27]. Similarly, the decidua
264 releases specific cytokines and alterations in these profiles may be associated with pregnancy
265 complications including miscarriage [28-33]. The decidua also responds to microbial infections via
266 the release of additional cytokines that function in innate defense [6, 34, 35]. However, in many
267 cases, these studies were performed on tissue explants that were multicellular in nature, thus
268 preventing an assessment of the contributions of cytokine release from distinct cell types. Similarly,
269 previous work utilizing tissue explants that are treated with recombinant cytokines, synthetic ligands
270 of various innate immune pathways, or infected with pathogens are also unable to define the
271 contributions of distinct cell types in these responses. The use of organoids therefore allows for
272 analyses of cellular responses to infection or innate immune activation from trophoblasts and
273 decidual glands in primary cell models that contain isolated cell types enriched at the maternal-fetal
274 interface. An additional strength of the TO model is that trophoblast stem cells can differentiate into
275 all three distinct trophoblast cell types comprising the human placenta [15], which is not possible in
276 many other existing models including isolation of CTBs from full-term placentas.

277 The constitutive release of IFN-λs from human trophoblasts is a highly unique phenomenon
278 that runs counter to much of what is understood about antiviral IFN signaling, which is centered on
279 a requirement for viral sensing to induce this pathway. Our findings from TOs support that IFN
280 release occurs soon after trophoblast differentiation and is likely an early mechanism used by the
281 placenta to defend from viral infections. Our study also indicates that TOs and DOs are largely

282 resistant to ZIKV infection and produced titers significantly lower than those observed in permissive
283 cells. Previous work has shown that human CTBs and EVTs are permissive to ZIKV whereas the
284 STB is resistant [7, 36]. Given that TOs contain EVTs, CTBs, and that the STB faces inward in the
285 organoid structure, it is possible that the low level of infection observed in TOs results from these
286 cells supporting ZIKV infection. It remains unknown whether EVTs and CTBs exhibit differential
287 responses to type III IFNs which might impact this differential susceptibility to ZIKV infection. The
288 mechanism of resistance of DOs is less clear, given that these organoids do not basally secrete the
289 type I and III IFNs we measured. Of note, DOs expressed high levels of many ISGs in the absence
290 of stimulation, which might be linked to their relative resistance to ZIKV infection. Interestingly, our
291 data also show that TOs constitutively release IFN-λ2 and that IFN-λ1 is only induced upon activation
292 of antiviral signaling pathways. IFN-λs genes are located in tandem on chromosome 19 in humans
293 and the mechanisms that might control the constitutive release of IFN-λ2 specifically in trophoblasts
294 is unclear. Our studies also show that type III IFNs are further induced by activation of antiviral innate
295 immune signaling in both TOs and DOs, with IFN-λ1 being the most induced cytokine detected in
296 both organoid types. However, the type I IFN IFN-β is induced to greater levels in TOs than DOs,
297 suggesting that at least some of the cells that comprise the maternal-fetal interface differentially rely
298 on type I and III IFNs for antiviral defenses.

299 Previous work suggests that type I IFNs damage placental structure and function in mice and
300 induce alterations in placental structure in *ex vivo* human chorionic villi [23]. In contrast, type III IFN
301 signaling in mice is protective against viral infections and there are no deleterious effects of treatment
302 of pregnant animals with recombinant IFN-λs [13, 14]. While the mechanisms for the opposing effects
303 of type I and III IFNs have yet to be fully elucidated, at least one ISG, interferon-induced
304 transmembrane (IFITM), inhibits fusion of CTBs into the STB [37, 38], which may indicate that
305 expression of select ISGs is tightly regulated to prevent IFN-mediated placental damage. Our data
306 in TOs and DOs suggests that trophoblasts and decidual cells exhibit differential responsiveness to

307 recombinant IFN treatment, with treatment of TOs inducing lower levels of ISGs than those observed
308 in DOs. While this might be attributed to reduced expression of the receptors associated with these
309 IFNs in TOs, there might also be additional mechanisms employed by trophoblasts to protect from
310 IFN- and ISG-mediated damage.

311 Our work presented here develops TOs and DOs from mid-to-late gestation placental tissue
312 and demonstrates that these organoids recapitulate some of the immunologic secretory phenotypes
313 of tissue explants isolated from matched placental tissue. We further show that TOs and DOs
314 constitutively secrete unique cytokines and respond to viral infections through the release of
315 organoid-specific cytokines. Our work also highlights the prominent role of type III IFNs in antiviral
316 immunity at the maternal-fetal interface and demonstrates that TOs constitutively release IFN-λ2.
317 Collectively, these studies define the differential responses of key cells comprising the maternal-fetal
318 interface and suggest that organoid-based models can be used to define innate immune signaling
319 at this interface.

320

321 **Materials and Methods**

322 **Human samples**. All human tissue used in this study was obtained through the UPMC Magee-
323 Womens Hospital Obstetric Maternal & Infant Database and Biobank after approval was received
324 from the University of Pittsburgh Institutional Review Board (IRB) and in accordance with the
325 guidelines of University of Pittsburgh human tissue procurement. Placental tissue used in this study
326 was collected from the second (23rd and 27th) and third (35th and 38th) trimesters, including from
327 dizygotic twins. Placental tissue was excluded for diagnosis of PPROM, labor, or maternal infection.

328

329 **Derivation and culture of trophoblast organoid (TOs) cultures from human placental samples**.
330 Villous trophoblast stem cells were isolated from fresh placental tissues as described previously [15].
331 Briefly, villi collected from fresh placental tissue were intensively washed, then were sequentially
332 digested with 0.2% trypsin-250 (Alfa Aesar, J63993-09)/0.02% EDTA (Sigma-Aldrich, E9884-100G)

333 and 1.0 mg/mL collagenase V (Sigma-Aldrich, C9263-100MG). Pooled digests were washed with
334 Advanced DMEM/F12 medium (Gibco 12634-010) and pelleted by centrifugation, then resuspended
335 in approximate 10 times volume of ice-cold growth-factor-reduced Matrigel (Corning 356231).
336 Matrigel "domes" (40 µl/well) were plated into 24-well tissue culture plates (Corning 3526), placed in
337 a 37°C incubator to pre-polymerize for ~2 min, turned upside down to ensure equal distribution of
338 the isolated cells in domes for another 10 min, then carefully overlaid with 500 µL prewarmed
339 trophoblast organoid medium (TOM) consisting of Advanced DMEM/F12 (Life Technologies, 12634-
340 010) supplemented with 1× B27 (Life Technologies, 17504-044), 1× N2 (Life Technologies, 17502-
341 048), 2 mM GlutaMAX™ supplement (Life Technologies, 35050-061), 100 µg/mL Primocin
342 (InvivoGen, ant-pm-1), 1.25 mM N-Acetyl-L-cysteine (Sigma, A9165), 500 nM A83-01 (Tocris, 2939),
343 1.5 µM CHIR99021 (Tocris, 4423), 50 ng/mL recombinant human EGF (Gibco, PHG0314), 80 ng/mL
344 recombinant human R-spondin 1 (R & D systems, 4645-RS-100), 100 ng/mL recombinant human
345 FGF2 (Peprotech, 100-18C), 50 ng/mL recombinant human HGF (Peprotech, 100-39), 10mM
346 nicotinamide (Sigma, N0636-100G), 2 µM Y-27632 (Sigma, Y0503-1MG), and 2.5 µM prostaglandin
347 E2 (PGE2, R & D systems, 22-961-0). Cultures were maintained in a 37°C humidified incubator with
348 5% CO_2. Medium was renewed every 2-3 days. Small trophoblast organoid spheroids became visible
349 by approximately day 12 post-isolation. Derived TOs were passaged every 10 to 14 days depending
350 on their size and density. To passage, TOs were released from domes with ice-cold cell recovery
351 solution (Corning, 354253) and then were digested in prewarmed TrypLE Express (Gibco, 12605-
352 028) or Stem Pro Accutase (Gibco, A11105-01) at 37°C for 5-7 min. Further mechanical dissociation
353 was achieved with an Eppendorf Explorer Plus electronic pipettes at its "mix" function setting by
354 pipetting up and down around 400 times through small-bore pipette tips. Dissociated TOs fragment
355 were collected and washed by centrifuge, then resuspended in fresh ice-cold Matrigel and replated
356 as domes at the desired density for continuous culture. For freezing TOs, overlaid TOM was
357 aspirated, TOs with Matrigel were resuspended in CryoStor CS10 stem cell freezing medium
358 (STEMCell Technologies, 07930) frozen at -80 ℃ and then transferred to liquid nitrogen for long-

359 term storage. For thawing cryopreserved TOs, TOs were thawed as quickly as possible, diluted with
360 5 times volume of basic TOM containing Advanced DMEM/F12, 2 mM GlutaMAX supplement, 10
361 mM HEPES (Gibco, 15630-106), 1 × Penicillin/Streptomycin (Lonza, 17-602E) and centrifuged to
362 pellet. Afterwards, TOs were resuspended in new ice-cold Matrigel and replated for recovery culture.
363

364 **Derivation and culture of decidual organoids (DOs) cultures from human decidua samples**.
365 Decidual gland-enriched cell suspension were acquired from fresh decidual tissue as described
366 previously [16, 39]. Briefly, isolated decidual tissues were cut into small pieces then digested in 1.25
367 U/mL Dispase II (Sigma, D4693)/0.4 mg/mL collagenase V (Sigma, C-9263) solution. Glandular cells
368 were filtered out from the digestion solution supernatant and resuspended in ice-cold Matrigel
369 (Corning, 356231), plated as domes in 24-well plates (Corning 3526), and finally overlaid with 500
370 μL prewarmed organoid Expansion Medium (ExM) with the same composition as previously
371 described[16]. The growth medium was renewed every 2-3 days. Mature organoids were passaged
372 by mechanically disruption following TrypLE Express (Gibco, 12605) digestion every 7-10 days.
373 Other maintenance were similar to those as previously described [39].
374

375 **Generation of TO and DO conditioned media (CM).** Overlaid TOM and ExM were collected every
376 2-4 days based on the growth status of TOs and DOs. Media from at least ten timepoints for each
377 established organoid lines were collected as TO-CM or DO-CM. Non-conditioned medium (NCM)
378 was TOM or ExM (described above) that had not been exposed to TOs or DOs, respectively.
379

380 **Cells and Viruses.** PHT cells were established and cultured as described previously [9] . Human
381 osteosarcoma U2OS (ATCC HTB-96) and Vero (ATCC CCL-81) cells were grown in Dulbecco's
382 minimal essential medium (DMEM) with 10% FBS and 1% antibiotic. JEG-3 and JAR were
383 purchased from the ATCC and cultured as previously described [9, 40]. HEK-Blue IFN-λ reporter
384 cells (hkb-ifnl) were purchased from InvivoGen and cultured according to the manufacturer's

385 instructions. ZIKV (Paraiba/2015, provided by David Watkins, University of Miami) was propagated
386 in Vero cells. Viral titers were determined by fluorescent focus assay as previously described [41]
387 using recombinant anti-double-stranded RNA monoclonal antibody J2 (provided by Abraham Brass,
388 University of Massachusetts) in Vero cells. Infection was determined by qRT-PCR as described
389 below. To assess antiviral activity, U2OS cells were exposed to TO or DO CM, or matched NCM, 24
390 hr prior to infection with ZIKV Paraiba/2015 for 72hrs. ZIKV infection of TOs and DOs was performed
391 using 10^6 FFU virus per well for 24-72hrs, as indicated.
392
393 **Immunofluorescence microscopy.** TOs and DOs were released from Matrigel domes with 1 mL of
394 cell recovery solution (Corning, 354253) per well without disrupting their 3D architecture, then were
395 fixed in 4%PFA for 30 min at room temperature, followed by 0.5% Triton X-100/PBS to permeabilize
396 for 30 min at 4°C. Organoids were washed and blocked in 5%(v/v) goat serum/0.1%(v/v) Tween-20
397 in PBS for 15 min at room temperature and then incubated with primary antibodies in the above-
398 described blocking solution at 4°C overnight. Organoids were then washed with PBS and then
399 incubated for 1-2 h at room temperature with Alexa Fluor-conjugated secondary antibodies
400 (Invitrogen). Organoids were washed again with PBS and mounted in Vectashield (Vector
401 Laboratories) containing 4′,6-diamidino- 2-phenylindole (DAPI) and were transferred onto
402 microscope slides with large-orifice 200 µL-tips (Fisher Scientific, 02707134). The following
403 antibodies or reagents were used: cytokeratin-7 (Abcam, ab9021), cytokeratin-19 (Abcam, ab9221),
404 E-cadherin (Invitrogen, PA5-85088), Abcam), Alexa Fluor 594–conjugated phalloidin (Invitrogen,
405 A12381), Alexa Fluor Plus 488 Goat anti-Mouse IgG secondary antibody (Invitrogen, A32723), Alexa
406 Fluor 488 Goat anti-Rabbit IgG secondary antibody (Invitrogen, A11034). Images were captured
407 using a Zeiss LSM 710 inverted laser scanning confocal microscope and contrast-adjusted in
408 Photoshop or Fiji.
409

410 **RNA extraction, cDNA synthesis and quantitative PCR.** Total RNA was extracted with the Sigma
411 GenElute total mammalian RNA miniprep kit following the manufacturer's instruction and using the
412 supplementary Sigma DNase digestion. RNA quality and concentration were determined using a
413 Nanodrop ND-1000 Spectrophotometer. Total RNA was reverse-transcribed with the iScript cDNA
414 synthesis kit (Bio-Rad) following the manufacturer's instructions. Quantitative PCR was performed
415 using the iQ SYBR Green Supermix (Bio-Rad, 1708882) on a CFX96 Touch Real-Time PCR
416 Detection System (Bio-Rad). Gene expression was determined based on a ΔC_T method normalized
417 to actin. The expression level of C19MC miRNAs hsa-miR-516b-5p, hsa-miR-517a-3p, hsa-miR-
418 525-5p and reference gene RNU6 was quantified by using the MystiCq® MicroRNA® Quantitation
419 System (Millipore Sigma) which includes miRNAs Poly(A) tailing, cDNA synthesis (MIRRT) and
420 miRNA qPCR (MIRRM00). MicroRNAs were first polyadenylated in a poly(A) polymerase reaction,
421 then reverse transcribed using an oligo-dT adapter primer according to the manufacturer's protocol
422 (Sigma-Aldrich, MIRRT). Individual microRNAs (microRNA-516b-5p, microRNA-517a-3p and
423 microRNA-525-5p) were quantified in real-time SYBR® Green RT-qPCR reactions with the specific
424 MystiCq microRNA qPCR Assay Primer (MIRAP00475, MIRAP00477 and MIRAP00512) and the
425 MystiCq Universal PCR Primer (MIRUP). Cq reading were normalized to the RNU6 internal reference
426 by the $2^{-\Delta Cq}$ method. Primer sequences for actin, IFN-β, IL-28A/IFN-λ2, IFI44L, OASL, GATA3,
427 MUC20, and ZKIV vRNA have been previously described [22, 42]. All primer sequences used in this
428 study can be found in Table S1.
429
430 **RNA-seq analysis**. For RNA-seq analysis, RNA was isolated from organoids as described above.
431 Purified Total RNA was verified by Thermo scientific Nanodrop one. The libraries were prepared by
432 the Duke Center for Genomic and Computational Biology (GCB) using the Tru-Seq stranded total
433 RNA prep kit (Illumina). Sequencing was performed on the NovaSeq 6000 by using 150-bp paired-
434 end sequencing. The reads were aligned to the human reference genome (GRCh38) using QIAGEN
435 CLC Genomics (v20) or the ZIKV genome to calculate the FPKM values. DESeq2 [43] was used to

436 normalized count data and to do the differential gene expression analysis with a significance cutoff
437 of 0.01 and a fold change cutoff of $\log_2(2)$. Heatmaps and hierarchical clustering was performed in
438 R using pheatmap package in R and were based on RPKM (reads per kilobase million). Files
439 associated with RNA-seq studies have been deposited into Sequence Read Archive under
440 accession number SRA. Data from PHT cells (accession SRP067137 and SRP109039) and JAR
441 (accession SRP095402) and JEG-3 cells (accession SRP109039) was based on published datasets
442 [9, 10, 44]. Principal component analyses were performed using pcaExplorer in R [45]. Volcano plots
443 were generated using the EnhancedVolcano package in R [46].
444
445 **hCG and PSG1 ELISAs and Luminex assays**. Human hCG (Sigma, RAB0092) and PSG1 (R&D
446 Systems, DY6799) ELISAs were performed according to the manufacturer's instructions. Plates
447 were read at 450 and 520 mm using a Synergy H1 microplate reader. All sample processing was
448 performed in duplicates and each experiment was performed with at least three biological replicates.
449 Luminex assays were performed using the following kits according to the manufacturer's instructions:
450 Bio-Plex Pro Human Inflammation Panel 1, 37-Plex kit (171AL001M; Bio-Rad Laboratories) and Bio-
451 Plex Pro Human Cytokine Screening Panel, 48-Plex kit (12007283; Bio-Rad Laboratories). The
452 plates were read on a MAGPIX (EMD Millipore) Luminex machine and analyzed using xPONENT
453 software (EMD Millipore).
454
455 **IFN-λ activity reporter assay.** For IFN-λ activity detection from CM, HEK-Blue IFN-λ reporter cells
456 were used according to the manufacture's protocol. Briefly, IFN-λ reporter cells were plated into a
457 96-well plate, then CM was added and incubated at 37 °C for 24 hr. Supernatants (20 µl) were
458 collected and then transferred into a 96-well plate and activity measured using QUANTI-Blue
459 Solution (InvivoGen, rep-qbs) after incubating at 37 °C for 2 hr using a spectrophotometer at 655 nm.
460 Each CM preparation was run in triplicate.
461

462 **Recombinant human IFN and poly(I:C) treatment.** For Poly (I:C) treatment, TOs or DOs were
463 incubated with 10 μg/mL Poly (I:C) diluted in organoid complete growth media for ~24 h, then
464 supernatant was collected for Luminex-based multianalyte profiling or RNA isolated as described for
465 qRT-PCR. For recombinant human IFN treatment, TOs or DOs were treated with IFN-β (8499-IF-
466 010; R&D Systems) or IFN-λ3 (5259-IL-025, R&D Systems) for 24 hr, then total RNA was extracted
467 as described above for following qRT-PCR analysis.
468
469 **Statistics and reproducibility.** All experiments reported in this study have been reproduced using
470 independent samples (tissues and organoids) from multiple donors. All statistical analyses were
471 performed using Prism software (GraphPad Software). Data are presented as mean ± SD, unless
472 otherwise stated. Statistical significance was determined as described in the figure legends.
473 Parametric tests were applied when data were distributed normally based on D'Agostino-Pearson
474 analyses; otherwise, nonparametric tests were applied. P values <0.05 were considered statistically
475 significant, with specific P values noted in the figure legends.
476
477 **Author contributions** LY designed and performed experiments and participated in manuscript
478 review and writing, CM performed tissue dissections and participated in manuscript review and
479 writing, and CC designed and performed experiments, participated in manuscript review and writing,
480 and secured funding.
481
482 **Acknowledgements**
483 We thank Jon Boyle (University of Pittsburgh) for careful review of the manuscript, Alexandra Wells
484 for assistance with bioinformatics, and the Magee Obstetric Maternal & Infant (MOMI) Database and
485 Biobank at the Magee Women's Research Institute (MWRI) for providing placental tissue. This
486 project was supported by NIH AI145828 (C.B.C.) and the Children's Hospital of Pittsburgh of the
487 UPMC Health System (C.B.C). This project also used the UPMC Hillman Cancer Center and Tissue

and Research Pathology/Pitt Biospecimen Core and Animal Facility shared resources which are supported in part by award P30CA047904.

514 **Literature Cited**

515

516 1. Burton GJ, Watson AL, Hempstock J, Skepper JN, Jauniaux E. Uterine glands provide
517 histiotrophic nutrition for the human fetus during the first trimester of pregnancy. J Clin Endocrinol
518 Metab. 2002;87(6):2954-9. Epub 2002/06/07. doi: 10.1210/jcem.87.6.8563. PubMed PMID:
519 12050279.

520 2. McDonagh S, Maidji E, Chang HT, Pereira L. Patterns of human cytomegalovirus infection in
521 term placentas: a preliminary analysis. J Clin Virol. 2006;35(2):210-5. Epub 2006/01/03. doi:
522 10.1016/j.jcv.2005.08.011. PubMed PMID: 16386950.

523 3. Weisblum Y, Panet A, Zakay-Rones Z, Haimov-Kochman R, Goldman-Wohl D, Ariel I, et al.
524 Modeling of human cytomegalovirus maternal-fetal transmission in a novel decidual organ culture. J
525 Virol. 2011;85(24):13204-13. Epub 2011/10/07. doi: 10.1128/JVI.05749-11. PubMed PMID:
526 21976654; PubMed Central PMCID: PMCPMC3233115.

527 4. Pereira L, Maidji E, McDonagh S, Genbacev O, Fisher S. Human cytomegalovirus
528 transmission from the uterus to the placenta correlates with the presence of pathogenic bacteria and
529 maternal immunity. J Virol. 2003;77(24):13301-14. Epub 2003/12/04. doi: 10.1128/jvi.77.24.13301-
530 13314.2003. PubMed PMID: 14645586; PubMed Central PMCID: PMCPMC296088.

531 5. Weisblum Y, Oiknine-Djian E, Vorontsov OM, Haimov-Kochman R, Zakay-Rones Z, Meir K,
532 et al. Zika Virus Infects Early- and Midgestation Human Maternal Decidual Tissues, Inducing Distinct
533 Innate Tissue Responses in the Maternal-Fetal Interface. J Virol. 2017;91(4). Epub 2016/12/16. doi:
534 10.1128/JVI.01905-16. PubMed PMID: 27974560; PubMed Central PMCID: PMCPMC5286880.

535 6. Guzeloglu-Kayisli O, Guo X, Tang Z, Semerci N, Ozmen A, Larsen K, et al. Zika Virus-
536 Infected Decidual Cells Elicit a Gestational Age-Dependent Innate Immune Response and
537 Exaggerate Trophoblast Zika Permissiveness: Implication for Vertical Transmission. J Immunol.
538 2020;205(11):3083-94. Epub 2020/11/04. doi: 10.4049/jimmunol.2000713. PubMed PMID:
539 33139490.

540 7. Platt DJ, Smith AM, Arora N, Diamond MS, Coyne CB, Miner JJ. Zika virus-related
541 neurotropic flaviviruses infect human placental explants and cause fetal demise in mice. Sci Transl
542 Med. 2018;10(426). Epub 2018/02/02. doi: 10.1126/scitranslmed.aao7090. PubMed PMID:
543 29386359; PubMed Central PMCID: PMCPMC6136894.

544 8. Rizzuto G, Tagliani E, Manandhar P, Erlebacher A, Bakardjiev AI. Limited Colonization
545 Undermined by Inadequate Early Immune Responses Defines the Dynamics of Decidual Listeriosis.
546 Infect Immun. 2017;85(8). Epub 2017/05/17. doi: 10.1128/IAI.00153-17. PubMed PMID: 28507070;
547 PubMed Central PMCID: PMCPMC5520438.

548 9. Bayer A, Lennemann NJ, Ouyang Y, Bramley JC, Morosky S, Marques ET, Jr., et al. Type III
549 Interferons Produced by Human Placental Trophoblasts Confer Protection against Zika Virus
550 Infection. Cell Host Microbe. 2016;19(5):705-12. Epub 2016/04/14. doi: 10.1016/j.chom.2016.03.008.
551 PubMed PMID: 27066743; PubMed Central PMCID: PMCPMC4866896.

552 10. Corry J, Arora N, Good CA, Sadovsky Y, Coyne CB. Organotypic models of type III interferon-
553 mediated protection from Zika virus infections at the maternal-fetal interface. Proc Natl Acad Sci U
554 S A. 2017;114(35):9433-8. Epub 2017/08/09. doi: 10.1073/pnas.1707513114. PubMed PMID:
555 28784796; PubMed Central PMCID: PMCPMC5584447.

556 11. Lazear HM, Schoggins JW, Diamond MS. Shared and Distinct Functions of Type I and Type
557 III Interferons. Immunity. 2019;50(4):907-23. Epub 2019/04/18. doi: 10.1016/j.immuni.2019.03.025.
558 PubMed PMID: 30995506; PubMed Central PMCID: PMCPMC6839410.

559 12. Wells AI, Coyne CB. Type III Interferons in Antiviral Defenses at Barrier Surfaces. Trends
560 Immunol. 2018;39(10):848-58. Epub 2018/09/17. doi: 10.1016/j.it.2018.08.008. PubMed PMID:
561 30219309; PubMed Central PMCID: PMCPMC6179363.

562 13. Jagger BW, Miner JJ, Cao B, Arora N, Smith AM, Kovacs A, et al. Gestational Stage and
563 IFN-lambda Signaling Regulate ZIKV Infection In Utero. Cell Host Microbe. 2017;22(3):366-76 e3.
564 Epub 2017/09/15. doi: 10.1016/j.chom.2017.08.012. PubMed PMID: 28910635; PubMed Central
565 PMCID: PMCPMC5647680.

566 14. Chen J, Liang Y, Yi P, Xu L, Hawkins HK, Rossi SL, et al. Outcomes of Congenital Zika
567 Disease Depend on Timing of Infection and Maternal-Fetal Interferon Action. Cell Rep.
568 2017;21(6):1588-99. Epub 2017/11/09. doi: 10.1016/j.celrep.2017.10.059. PubMed PMID:
569 29117563; PubMed Central PMCID: PMCPMC5726784.

570 15. Turco MY, Gardner L, Kay RG, Hamilton RS, Prater M, Hollinshead MS, et al. Trophoblast
571 organoids as a model for maternal-fetal interactions during human placentation. Nature.
572 2018;564(7735):263-7. Epub 2018/11/30. doi: 10.1038/s41586-018-0753-3. PubMed PMID:
573 30487605; PubMed Central PMCID: PMCPMC7220805.

574 16. Turco MY, Gardner L, Hughes J, Cindrova-Davies T, Gomez MJ, Farrell L, et al. Long-term,
575 hormone-responsive organoid cultures of human endometrium in a chemically defined medium. Nat
576 Cell Biol. 2017;19(5):568-77. Epub 2017/04/11. doi: 10.1038/ncb3516. PubMed PMID: 28394884;
577 PubMed Central PMCID: PMCPMC5410172.

578 17. Sheridan MA, Fernando RC, Gardner L, Hollinshead MS, Burton GJ, Moffett A, et al.
579 Establishment and differentiation of long-term trophoblast organoid cultures from the human
580 placenta. Nat Protoc. 2020;15(10):3441-63. Epub 2020/09/11. doi: 10.1038/s41596-020-0381-x.
581 PubMed PMID: 32908314.

582 18. Okae H, Toh H, Sato T, Hiura H, Takahashi S, Shirane K, et al. Derivation of Human
583 Trophoblast Stem Cells. Cell Stem Cell. 2018;22(1):50-63 e6. Epub 2017/12/19. doi:
584 10.1016/j.stem.2017.11.004. PubMed PMID: 29249463.

585 19. Haider S, Meinhardt G, Saleh L, Kunihs V, Gamperl M, Kaindl U, et al. Self-Renewing
586 Trophoblast Organoids Recapitulate the Developmental Program of the Early Human Placenta.
587 Stem Cell Reports. 2018;11(2):537-51. Epub 2018/08/07. doi: 10.1016/j.stemcr.2018.07.004.
588 PubMed PMID: 30078556; PubMed Central PMCID: PMCPMC6092984.

589 20. Marinic M, Rana S, Lynch VJ. Derivation of endometrial gland organoids from term placenta.
590 Placenta. 2020;101:75-9. Epub 2020/09/17. doi: 10.1016/j.placenta.2020.08.017. PubMed PMID:
591 32937244.

592 21. Mouillet JF, Ouyang Y, Coyne CB, Sadovsky Y. MicroRNAs in placental health and disease.
593 Am J Obstet Gynecol. 2015;213(4 Suppl):S163-72. Epub 2015/10/03. doi:
594 10.1016/j.ajog.2015.05.057. PubMed PMID: 26428496; PubMed Central PMCID:
595 PMCPMC4592520.

596 22. Megli C, Morosky S, Rajasundaram D, Coyne CB. Inflammasome signaling in human
597 placental trophoblasts regulates immune defense against Listeria monocytogenes infection. J Exp
598 Med. 2021;218(1). Epub 2020/09/26. doi: 10.1084/jem.20200649. PubMed PMID: 32976558.

599 23. Yockey LJ, Jurado KA, Arora N, Millet A, Rakib T, Milano KM, et al. Type I interferons instigate
600 fetal demise after Zika virus infection. Sci Immunol. 2018;3(19). Epub 2018/01/07. doi:
601 10.1126/sciimmunol.aao1680. PubMed PMID: 29305462; PubMed Central PMCID:
602 PMCPMC6049088.

603 24. Ander SE, Rudzki EN, Arora N, Sadovsky Y, Coyne CB, Boyle JP. Human Placental
604 Syncytiotrophoblasts Restrict Toxoplasma gondii Attachment and Replication and Respond to
605 Infection by Producing Immunomodulatory Chemokines. mBio. 2018;9(1). Epub 2018/01/11. doi:
606 10.1128/mBio.01678-17. PubMed PMID: 29317509; PubMed Central PMCID: PMCPMC5760739.

607 25. Liu J, Hao S, Chen X, Zhao H, Du L, Ren H, et al. Human placental trophoblast cells
608 contribute to maternal-fetal tolerance through expressing IL-35 and mediating iTR35 conversion. Nat
609 Commun. 2019;10(1):4601. Epub 2019/10/12. doi: 10.1038/s41467-019-12484-z. PubMed PMID:
610 31601798; PubMed Central PMCID: PMCPMC6787064.

611 26. Vassiliadis S, Ranella A, Papadimitriou L, Makrygiannakis A, Athanassakis I. Serum levels
612 of pro- and anti-inflammatory cytokines in non-pregnant women, during pregnancy, labour and
613 abortion. Mediators Inflamm. 1998;7(2):69-72. Epub 1998/12/04. doi: 10.1080/09629359891199.
614 PubMed PMID: 9836491; PubMed Central PMCID: PMCPMC1781827.

615 27. Benyo DF, Smarason A, Redman CW, Sims C, Conrad KP. Expression of inflammatory
616 cytokines in placentas from women with preeclampsia. J Clin Endocrinol Metab. 2001;86(6):2505-
617 12. Epub 2001/06/09. doi: 10.1210/jcem.86.6.7585. PubMed PMID: 11397847.

618 28. Lash GE, Ernerudh J. Decidual cytokines and pregnancy complications: focus on
619 spontaneous miscarriage. J Reprod Immunol. 2015;108:83-9. Epub 2015/03/17. doi:
620 10.1016/j.jri.2015.02.003. PubMed PMID: 25771398.

621 29. von Rango U, Classen-Linke I, Raven G, Bocken F, Beier HM. Cytokine microenvironments
622 in human first trimester decidua are dependent on trophoblast cells. Fertil Steril. 2003;79(5):1176-
623 86. Epub 2003/05/10. doi: 10.1016/s0015-0282(02)04829-x. PubMed PMID: 12738514.

624 30. Alam SM, Konno T, Sahgal N, Lu L, Soares MJ. Decidual cells produce a heparin-binding
625 prolactin family cytokine with putative intrauterine regulatory actions. J Biol Chem.
626 2008;283(27):18957-68. Epub 2008/05/10. doi: 10.1074/jbc.M801826200. PubMed PMID:
627 18467328; PubMed Central PMCID: PMCPMC2441551.

628 31. Denison FC, Kelly RW, Calder AA, Riley SC. Cytokine secretion by human fetal membranes,
629 decidua and placenta at term. Hum Reprod. 1998;13(12):3560-5. Epub 1999/01/14. doi:
630 10.1093/humrep/13.12.3560. PubMed PMID: 9886550.

631 32. Laham N, Brennecke SP, Rice GE. Interleukin-8 release from human gestational tissue
632 explants: the effects of lipopolysaccharide and cytokines. Biol Reprod. 1997;57(3):616-20. Epub
633 1997/09/01. doi: 10.1095/biolreprod57.3.616. PubMed PMID: 9282999.

634 33. Pitman H, Innes BA, Robson SC, Bulmer JN, Lash GE. Altered expression of interleukin-6,
635 interleukin-8 and their receptors in decidua of women with sporadic miscarriage. Hum Reprod.
636 2013;28(8):2075-86. Epub 2013/06/07. doi: 10.1093/humrep/det233. PubMed PMID: 23739222.

637 34. Qiu X, Zhu L, Pollard JW. Colony-stimulating factor-1-dependent macrophage functions
638 regulate the maternal decidua immune responses against Listeria monocytogenes infections during
639 early gestation in mice. Infect Immun. 2009;77(1):85-97. Epub 2008/10/15. doi: 10.1128/IAI.01022-
640 08. PubMed PMID: 18852237; PubMed Central PMCID: PMCPMC2612255.

641 35. Barber EM, Fazzari M, Pollard JW. Th1 cytokines are essential for placental immunity to
642 Listeria monocytogenes. Infect Immun. 2005;73(10):6322-31. Epub 2005/09/24. doi:
643 10.1128/IAI.73.10.6322-6331.2005. PubMed PMID: 16177303; PubMed Central PMCID:
644 PMCPMC1230899.

645 36. Tabata T, Petitt M, Puerta-Guardo H, Michlmayr D, Wang C, Fang-Hoover J, et al. Zika Virus
646 Targets Different Primary Human Placental Cells, Suggesting Two Routes for Vertical Transmission.
647 Cell Host Microbe. 2016;20(2):155-66. Epub 2016/07/23. doi: 10.1016/j.chom.2016.07.002. PubMed
648 PMID: 27443522; PubMed Central PMCID: PMCPMC5257282.

649 37. Buchrieser J, Degrelle SA, Couderc T, Nevers Q, Disson O, Manet C, et al. IFITM proteins
650 inhibit placental syncytiotrophoblast formation and promote fetal demise. Science.
651 2019;365(6449):176-80. Epub 2019/07/13. doi: 10.1126/science.aaw7733. PubMed PMID:
652 31296770.

653 38. Zani A, Zhang L, McMichael TM, Kenney AD, Chemudupati M, Kwiek JJ, et al. Interferon-
654 induced transmembrane proteins inhibit cell fusion mediated by trophoblast syncytins. J Biol Chem.
655 2019;294(52):19844-51. Epub 2019/11/19. doi: 10.1074/jbc.AC119.010611. PubMed PMID:
656 31735710; PubMed Central PMCID: PMCPMC6937555.

657 39. Turco M, Gardner, L., Koo, B., Moffett, A., & Burton, G. Derivation and long-term expansion
658 of human endometrial and decidual organoids. Protocol Exchange. 2017. doi:
659 10.1038/protex.2017.030.

660 40. Drummond CG, Nickerson CA, Coyne CB. A Three-Dimensional Cell Culture Model To Study
661 Enterovirus Infection of Polarized Intestinal Epithelial Cells. mSphere. 2016;1(1). Epub 2016/06/16.
662 doi: 10.1128/mSphere.00030-15. PubMed PMID: 27303677; PubMed Central PMCID:
663 PMCPMC4863623.

664 41. Payne AF, Binduga-Gajewska I, Kauffman EB, Kramer LD. Quantitation of flaviviruses by
665 fluorescent focus assay. J Virol Methods. 2006;134(1-2):183-9. Epub 2006/03/03. doi:
666 10.1016/j.jviromet.2006.01.003. PubMed PMID: 16510196.

667 42. Good C, Wells AI, Coyne CB. Type III interferon signaling restricts enterovirus 71 infection of
668 goblet cells. Sci Adv. 2019;5(3):eaau4255. Epub 2019/03/12. doi: 10.1126/sciadv.aau4255. PubMed
669 PMID: 30854425; PubMed Central PMCID: PMCPMC6402847.

670 43. Love MI, Huber W, Anders S. Moderated estimation of fold change and dispersion for RNA-
671 seq data with DESeq2. Genome Biol. 2014;15(12):550. Epub 2014/12/18. doi: 10.1186/s13059-014-
672 0550-8. PubMed PMID: 25516281; PubMed Central PMCID: PMCPMC4302049.

673 44. Van Twisk D, Murphy SP, Thakar J. Optimized logic rules reveal interferon-gamma-induced
674 modes regulated by histone deacetylases and protein tyrosine phosphatases. Immunology.
675 2017;151(1):71-80. Epub 2017/01/06. doi: 10.1111/imm.12707. PubMed PMID: 28054346; PubMed
676 Central PMCID: PMCPMC5382347.

677 45. Marini F, Binder H. Available from:
678 https://www.bioconductor.org/packages/release/bioc/vignettes/pcaExplorer/inst/doc/pcaExplorer.ht
679 ml.

680 46. Blighe K, Rana S, Lewis M. EnhancedVolcano: Publication-ready volcano plots with
681 enhanced colouring and labeling. R package version 1.10.0 2021. Available from:
682 https://github.com/kevinblighe/EnhancedVolcano.
683

684

685

686

687

688

689

690

691

692

Figure 1

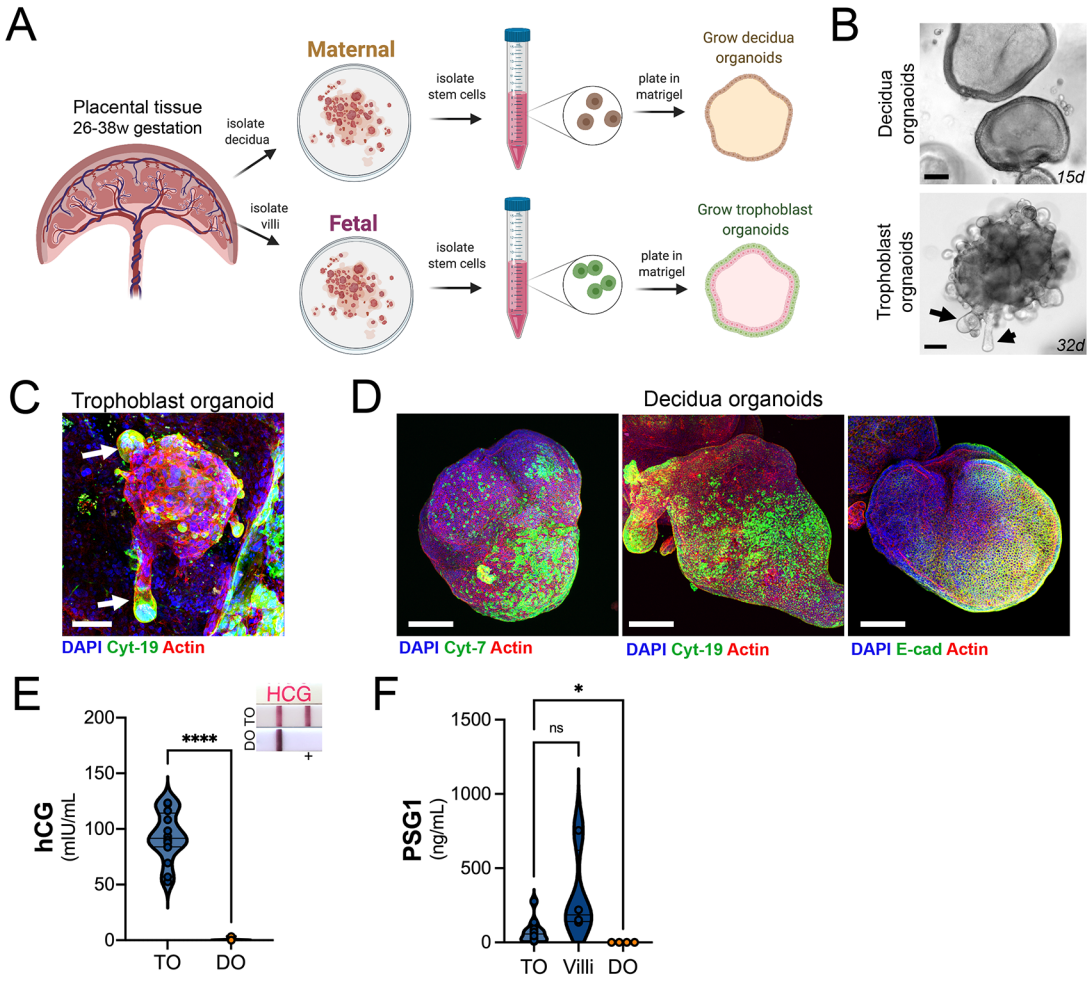

Figure 1. Long-term three-dimensional organoids cultures can be established from human mid- and late-gestation trophoblasts and decidua. (A) Schematic representation of the derivation of trophoblast organoids (TOs) and decidual organoids (DOs) from placental tissue. **(B)** Representative bright-field images of TOs and DOs after passaging in complete growth medium TOM and ExM, respectively at 15 days (DO, top) or 32 days (bottom) post-passaging . Scale bar, 50 µm. Black arrows denote placental-like villi extending from TOs (bottom). **(C)** Confocal microscopy for cytokeratin-19 (Cyt-19, green), and actin (red) in a TO. DAPI-stained nuclei are in blue. Scale bar, 50 µm. White arrows denote placental-like villi. **(D)** Confocal microscopy for cytokeratin-7 (cyt-7, green, left), cytokeratin-19 (Cyt-19, green, middle), or E-cadherin (E-cad, grren, right) and actin (red in all) in DOs. DAPI-stained nuclei are in blue. Scale bar, 50 µm. **(E)** Levels of hCG in conditioned medium (CM) isolated from TOs (blue) or DOs (orange) as determined by ELISA. Each symbol represents an individual CM preparation. Upper right shows the OTC pregnancy test stripe denoting an hCG positive line in TOs, but not DOs, after being placed into CM. **(F)** Levels of PSG-1 in conditioned medium (CM) isolated from TOs (light blue), chorionic villous explants (dark blue), or DOs (orange) as determined by ELISA. In (E) and (F) each symbol represents an individual CM

714 preparation and significance was determined by Mann-Whitney U test. ****, $P < 0.0001$, * $P<0.05$,
715 ns, not significant.
716
717
718
719
720
721
722
723
724
725
726
727
728
729
730
731
732
733
734
735
736
737
738
739
740
741
742

743 **Figure 2**

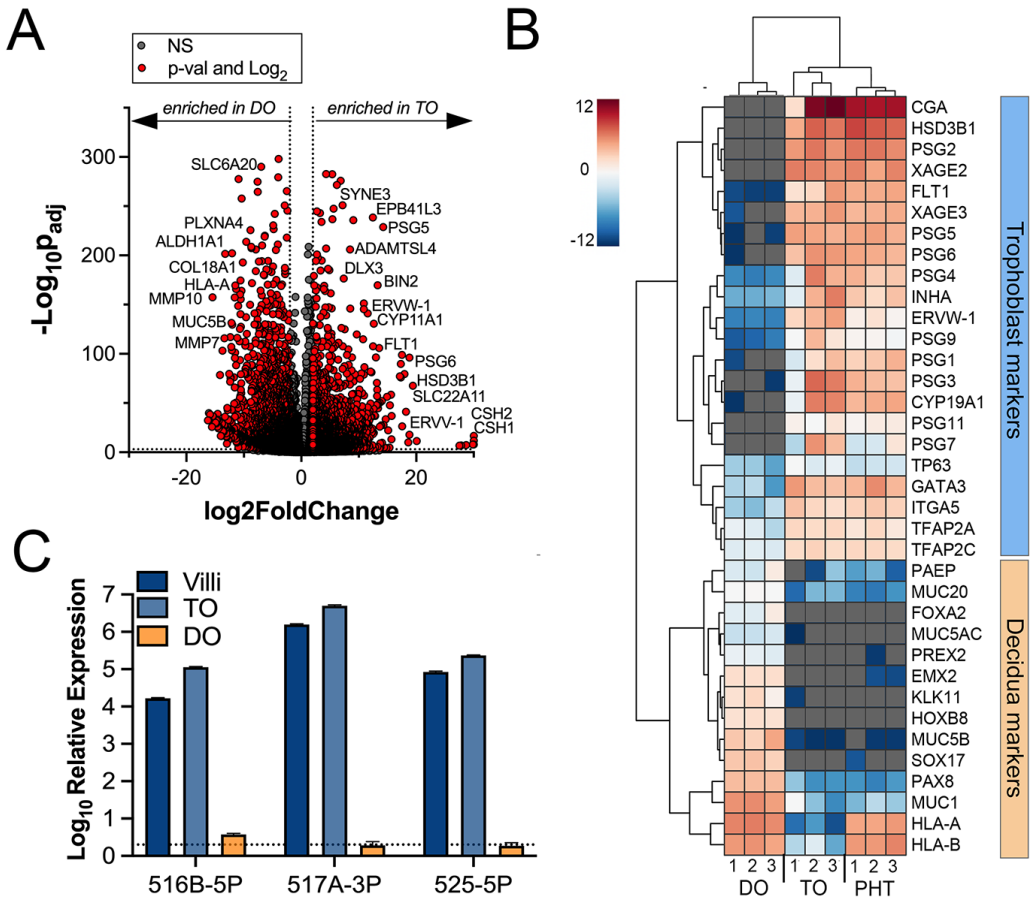

744

745 **Figure 2. Whole genome transcriptional profiling of trophoblast and decidua organoids. (A),**
746 Volcano plot demonstrating differentially expressed transcripts in trophoblast organoids (TOs) or
747 decidua organoids (DOs) as assessed by DeSeq2 analysis. Grey circles represent genes whose
748 expression was not significantly changes and red denotes transcripts significantly enriched in TOs
749 (right) or DOs (left) (significance was set at $p<0.01$ and log2 fold-change of +/- 2). **(B),** Heatmap
750 (based on log2 RPKM values) of transcripts expressed in DOs, TOs, or primary human trophoblasts
751 (PHT) cells that are associated with markers of trophoblasts (top, blue) or the decidua (bottom,
752 orange). Key at left. Red indicates high levels of expression, blue indicates low levels of expression,
753 and grey indicates no reads detected. Hierarchical clustering is shown at top**. (C),** Expression of
754 three members of the C19MC family (miR-516-5p, 517A-3p, and 525-5p) in TOs (light blue) and DOs
755 (orange), or in chorionic villi (dark blue) isolated from human placentas.
756

757

758

759

Figure 3

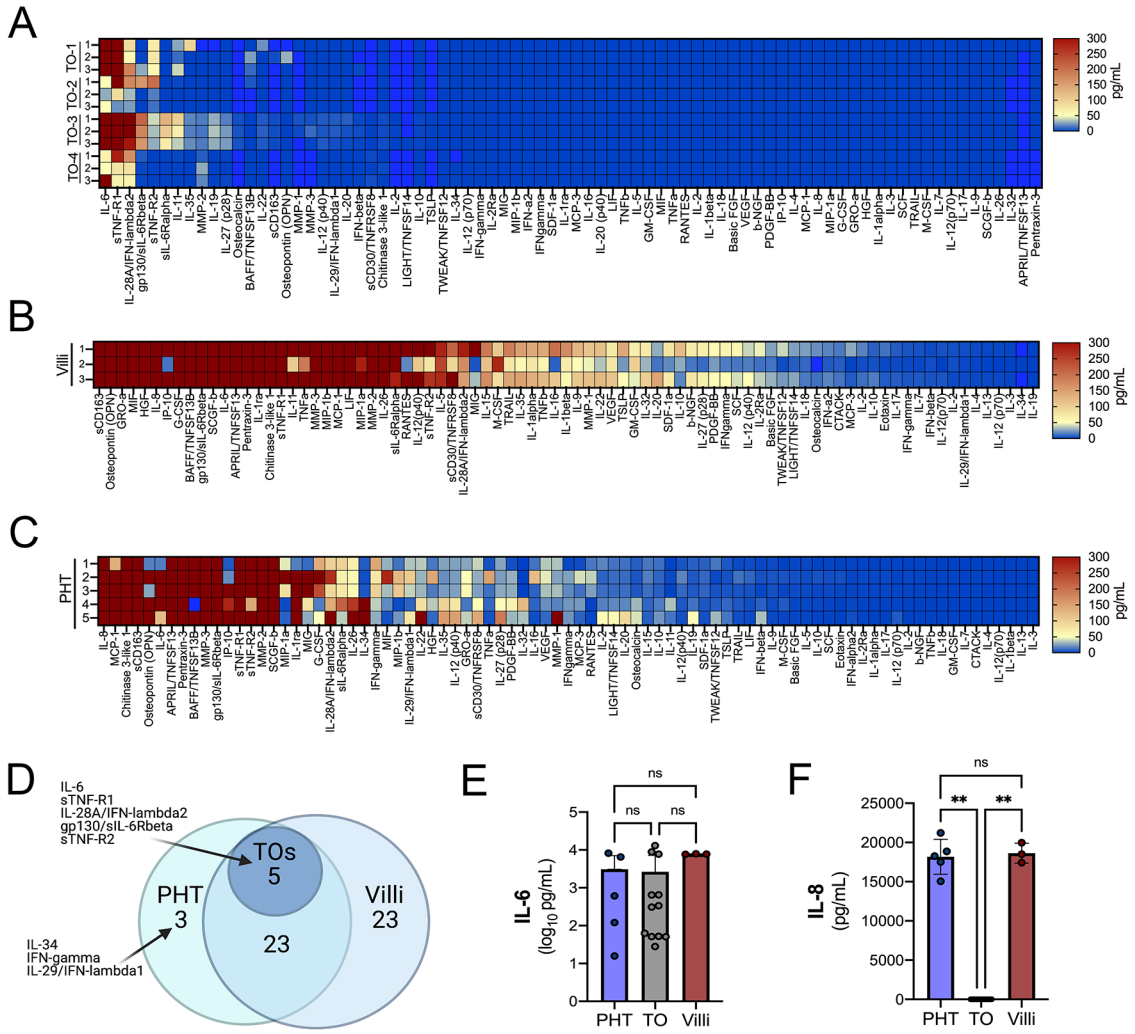

Figure 3. Cytokine secretion profiles from trophoblast organoids, matched placenta tissue, and primary cells. **(A)** Heatmap of twelve conditioned medium (CM) preparations generated from established TO lines analyzed by Luminex-based multianalyte profiling for the indicated cytokines, chemokines, and growth factors. Scale is shown at right. **(B)** Heatmap of CM generated from placental chorionic villi explants matched to TOs shown in A. Luminex assays were performed from three independent CM preparations. Scale is shown at right. **(C)** Heatmap of CM generated from primary human trophoblast cells cultured from full-term placentas. Luminex assays were performed from five independent CM preparations. Scale is at right. **(D)** Venn diagram showing the overlap of detectable factors in TOs, matched placenta chorionic villi, and primary cells from A-C. **(E, F)** Concentrations and comparison of the levels of IL-6 (E) and IL-8 (F) in CM from TOs (grey), matched chorionic villi (dark red), and primary cells (blue) shown in A-C. Each symbol represents a unique CM preparation. Significance was determined by Kruskal Wallace U test with multiple comparisons. **, $P < 0.01$; ns, not significant.

Figure 4

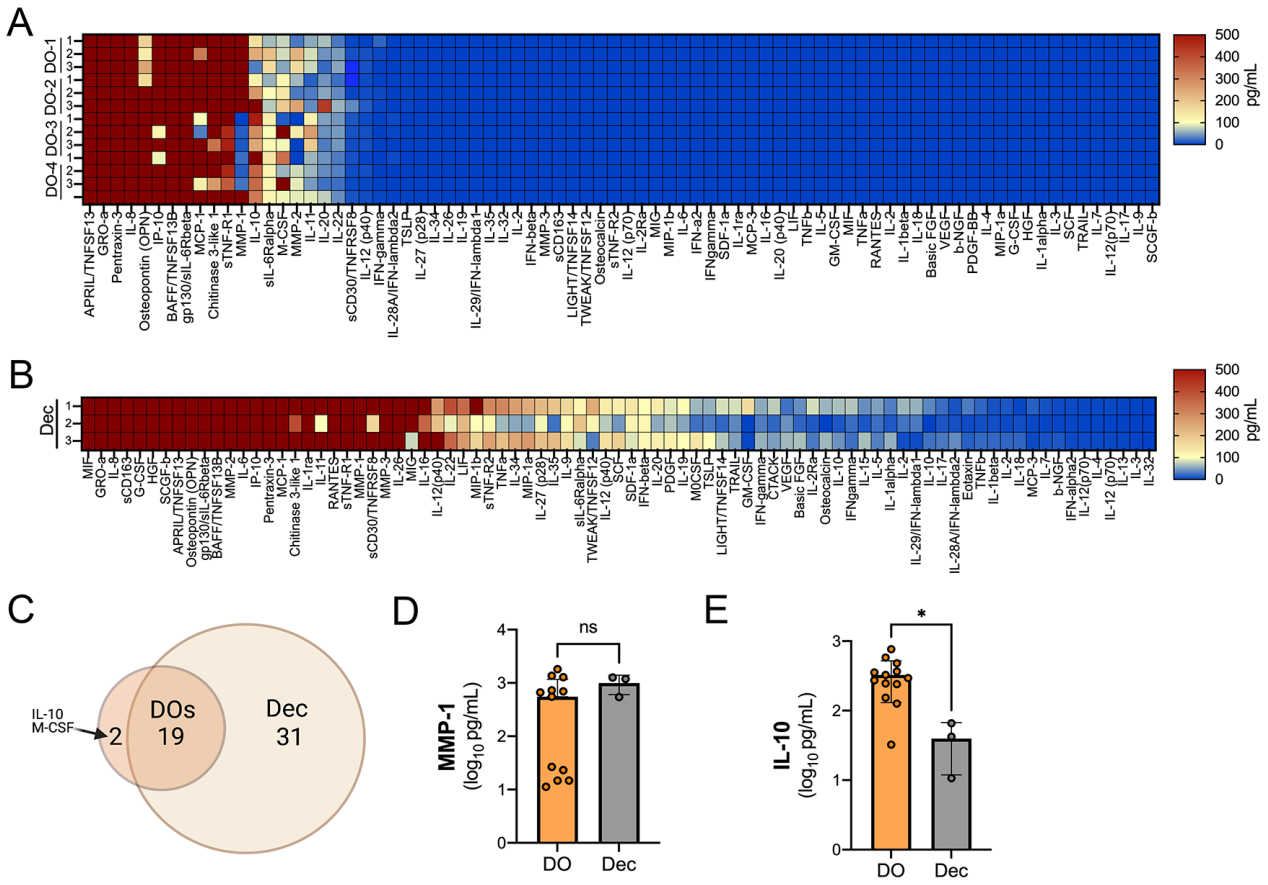

Figure 4. Cytokine secretion profiles from decidua organoids and decidua tissue. **(A)** Heatmap of twelve CM preparations generated from established DO lines analyzed by Luminex-based multianalyte profiling. Scale is at right. **(B)** Heatmap of CM generated from three independent decidual explants (two of these, at top and middle, are matched to DOs shown in A). Luminex assays were performed from three independent CM preparations. Scale is shown at right. **(C)** Venn diagram showing the overlap of detectable factors in CM isolated from DOs and decidual tissues. **(D, E)** Concentrations and comparison of the levels of MMP-1 (D) and IL-10 (E) in CM from DOs (orange) and decidual tissues (grey) shown in A and B. Each symbol represents a unique CM preparation. Significance was determined by Mann-Whitney U test. *, $P < 0.05$; ns, not significant.

794 **Figure 5**

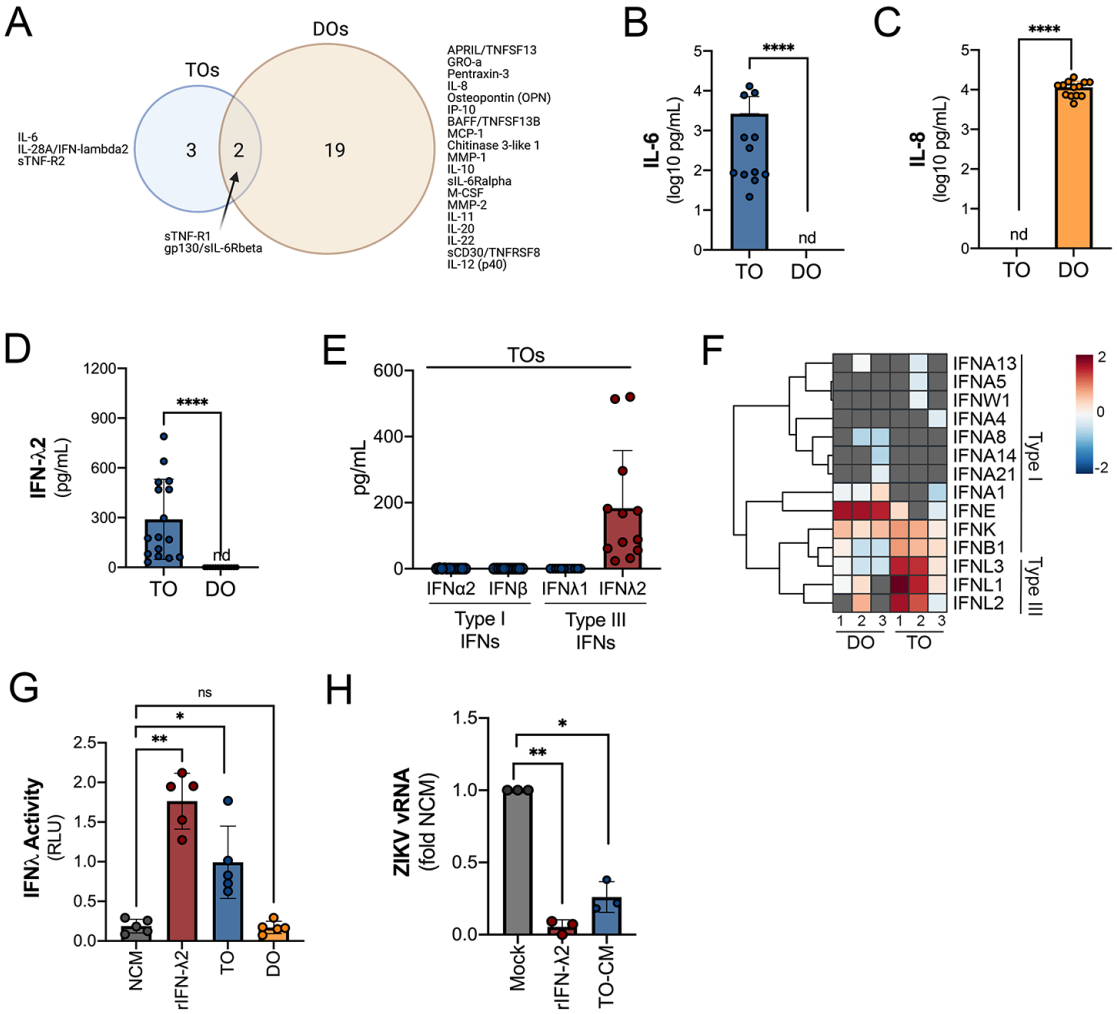

795

796 **Figure 5. Trophoblast organoids preferentially secrete high levels of antiviral IFN-λ2**. **(A)** Venn
797 diagram comparing the factors identified in CM isolated from TOs and DOs. **(B, C)** Concentrations
798 and comparison of the levels of IL-6 (B) and IL-8 (C) released by TOs (blue) and DOs (orange)
799 determined by Luminex-based profiling. Each symbol represents a unique CM preparation. **(D)**
800 Comparison of the levels of IFN-λ2 in CM isolated from TOs (blue) and DOs (orange) as determined
801 by Luminex. **(E)** Comparison of the levels of the type I IFNs IFN-α2 and IFN-β and type III IFNs IFN-
802 λ1 and IFN-λ2 in CM isolated from TOs. **(F),** Heatmap (based on log2 RPKM values) of transcripts
803 associated with type I (top) or III (bottom) IFNs in TOs or DOs. Key at right. Red indicates high levels
804 of expression, blue indicates low levels of expression, and grey indicates no reads detected. **(G)**
805 IFN-λ activity of CM isolated from TOs (blue) and DOs (orange) as assessed using an IFN-λ reporter
806 293T cells line. NCM (non-conditioned medium, grey) was as negative control, NCM supplemented
807 with recombinant human IFN-λ2 (100ng) was used as a positive control (red). **(H)** Human
808 osteosarcoma U2OS cells were treated with CM isolated from TOs (blue) or with recombinant IFN-
809 λ2 (100ng) for 24hrs and then infected with ZIKV for 24hrs (in the presence of CM). Level of ZIKV
810 replication was assessed by viral RNA as determined by qPCR. Data are shown as fold change from
811 NCM and from at least three independent CM preparations. Significance was determined by Mann-

Whitney U test or by Kruskal Wallace U test with multiple comparisons. *, $P < 0.05$; **, $P < 0.01$; ****, $P < 0.0001$. In D-E,G–H, each symbol represents unique CM preparations.

839 **Figure 6**

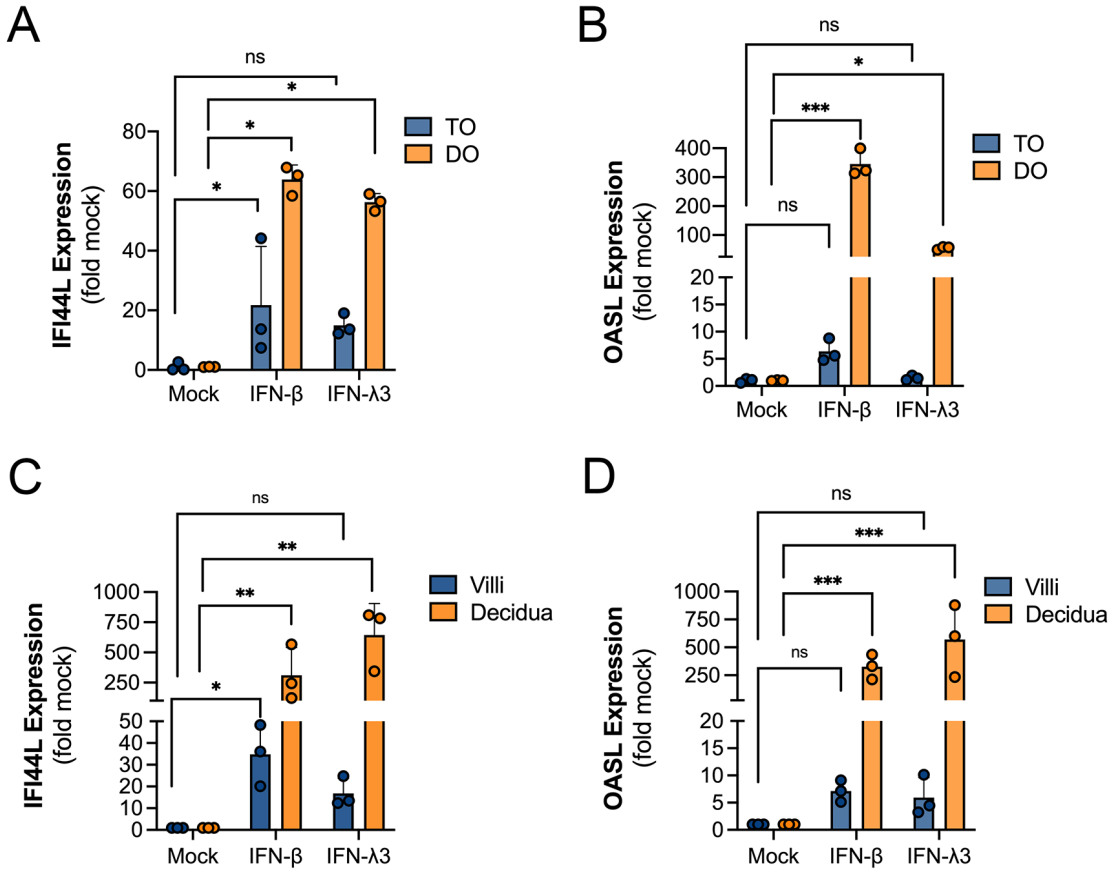

840

841 **Figure 6**. **Responses of TOs and DOs and placental tissue to recombinant IFNs. (A, B)** RT-
842 qPCR analyses for two ISGs, IFI44L (A) and OASL(B) in TOs (blue) and DOs (orange) treated with
843 100ng recombinant human IFN-β or IFN-λ3 treatment for ~24 hours. Data are shown as fold change
844 from mock-treated controls two independent replicates performed in triplicate. **(C, D),** RT-qPCR
845 analyses for IFI44L (C) and OASL(D) in chorionic villous (blue) or decidua (orange) explants treated
846 100ng recombinant human IFN-β or IFN-λ3 treatment for ~24 hours. Significance was determined
847 by Kruskal Wallace U test with multiple comparisons. *, $P < 0.05$; ***; ** $P < 0.01$; $P < 0.001$; ns, not
848 significant.
849

850

851

852

853

854

855 **Figure 7**

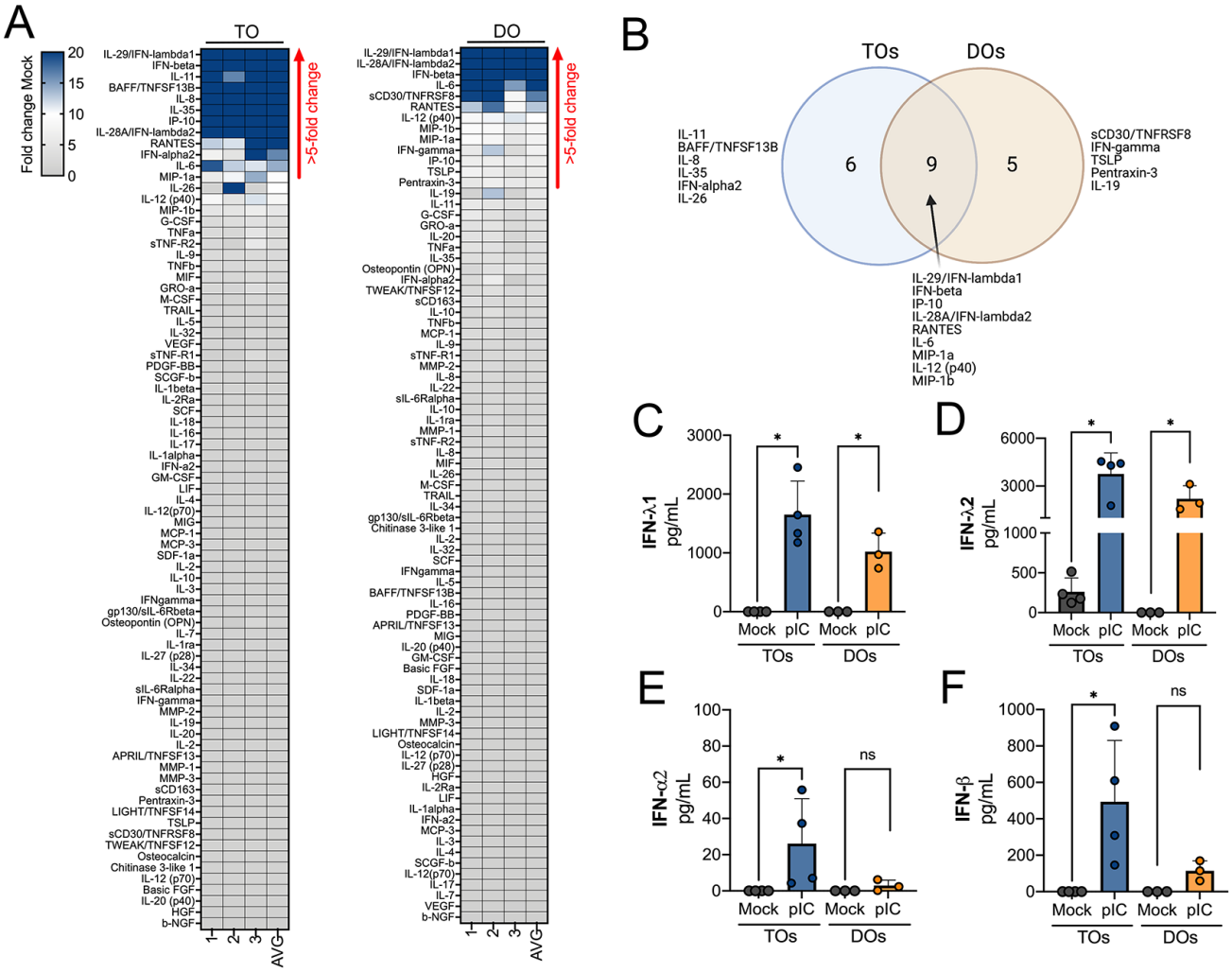

856

857 **Figure 7. Differential cytokine release in TOs and DOs treated with poly I:C. (A)** Heatmaps
858 demonstrating the induction of factors at left (shown as fold change from mock-treated controls) from
859 TOs (left panel) and DOs (right panel) treated with 10μg poly (I:C) and analyzed by multiplex
860 Luminex-based profiling. AVG denotes the average change in concentration of factors over CMs
861 from individual preparations. Dark blue denotes significantly induced factors compared with
862 untreated controls. Gray or white denotes little to no change (scale at top left). The red arrow
863 demonstrates factors with induction greater than five-fold change observed in the average of
864 separate experiments. Data are from four individual CM preparations from at least two unique
865 matched organoid lines. **(B)** Venn diagram showing overlap of the factors released >5-fold by poly
866 I:C treatment in TOs and DOs. **(C-F)** Levels of IFN-λ1 (C), IFN-λ2 (D) IFN-α2 (E), and IFN-β (F) in
867 CM isolated from poly I:C-treated TOs (blue) and DOs (orange) or in mock-treated controls (grey).
868 In C-F, each symbol represents individual CM preparations. In C-F significance was determined
869 using a Mann-Whitney U test. *, $P < 0.05$; ns, not significant.
870

871

872 **Figure 8**

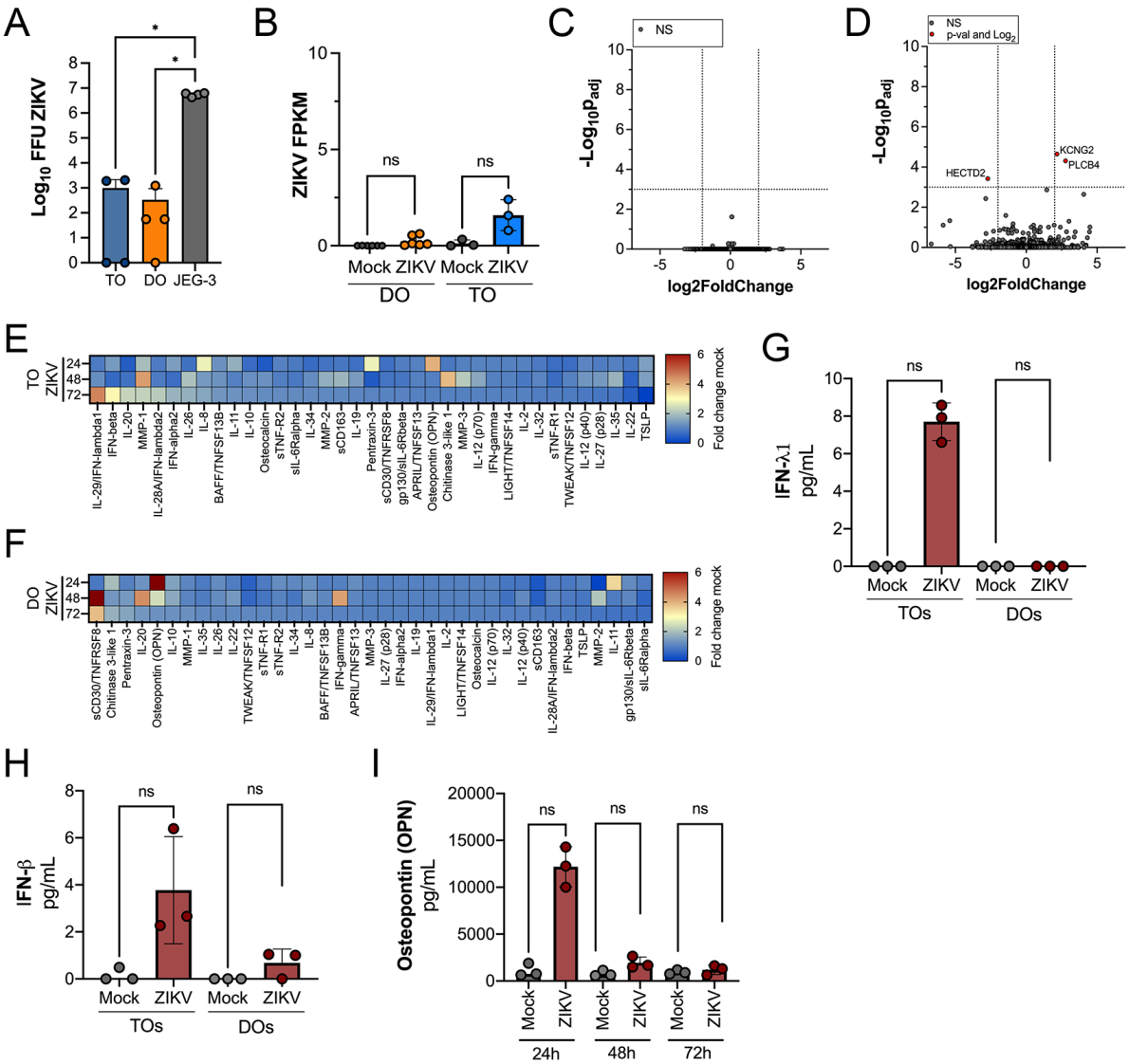

873

874 **Figure 8**. **Differential cytokine release in TOs and DOs infected with ZIKV**. **(A)** ZIKV infection as
875 assessed by FFU assays in TOs (blue), DOs (orange), or JEG-3 cells (grey) infected with ZIKV for
876 72hrs. **(B)** Presence of ZIKV viral RNA (based on FPKM values) from mock- or ZIKV-infected DOs
877 (left) or TOs (right) as assessed by RNA-Seq. **(C, D)** Volcano plots demonstrating differentially
878 expressed transcripts in mock versus ZIKV infected DOs (C) or TOs (D) as assessed by DeSeq2.
879 Grey circles represent genes whose expression was not significantly changes and red denotes
880 transcripts significantly enriched in TOs (right) or DOs (left) (significance was set at $p<0.05$ and log2
881 fold-change of +/- 2). **(E, F)** Heatmaps demonstrating the induction of cytokines in CM (shown as
882 fold change from mock controls) collected from TOs (E) and DOs (F) infected with ZIKV for indicated
883 hours (24 to 72 hours) analyzed by multiplex Luminex-based profiling. Scale is shown at right. **(G,**
884 **H**) Concentrations of IFN-λ1 (G) and IFN-β (H) in CM generated from TOs and DOs infected with
885 ZIKV for 72 hrs (dark red) or in mock-treated controls (grey). **(I)** Concentrations of osteopontin in CM
886 generated from DOs infected with ZIKV for the indicated time (dark red) or in mock infected controls

887 (mock, grey). In G-I, each symbol represents individual CM preparation. Significance was determined
888 with Mann-Whitney U test. ns, not significant.
889
890
891
892
893
894
895
896
897
898
899
900
901
902
903
904
905
906
907
908
909
910
911
912
913

914 **Supplemental Figure 1**

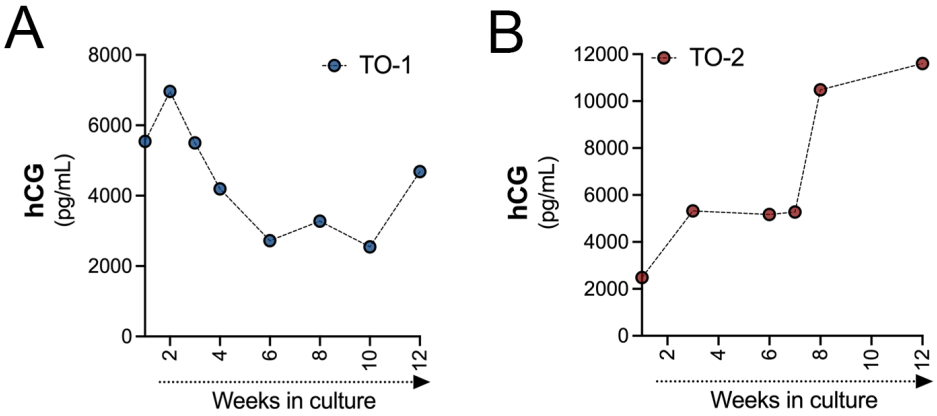

915

916 **Supplemental Figure 1. (A,B)** hCG levels as assessed by ELISA in conditioned medium isolated
917 from two TOs lines isolated at the indicated weeks during culture.

918

919

920

921

922

923

924

925

926

927

928

929

930

931

932

933

934

935 **Supplemental Figure 2**

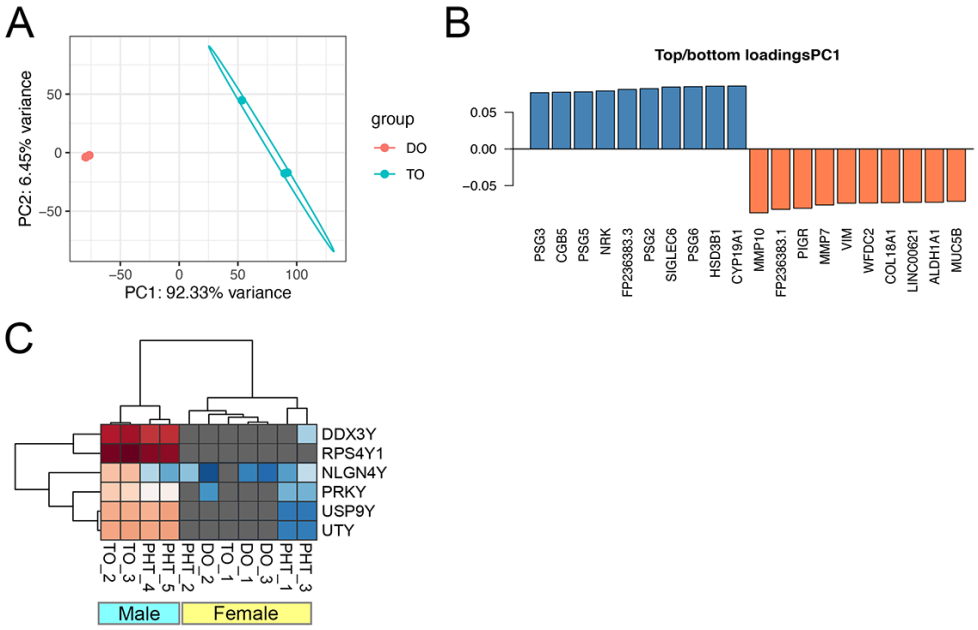

936

937

938 **Supplemental Figure 2. RNASeq of TOs and DOs. . (A)** Principal component analysis based on
939 transcriptional profiles from DOs (orange) or TOs (blue**). (B)** Transcripts on the first principal
940 component (PC1) with the greatest variance. Blue indicates enrichment in TOs and orange
941 indicates enrichment in DOs. **(C)** Heatmap (based on log2 RPKM values) of representative Y-linked
942 transcripts in TOs, DOs, or primary human trophoblasts (PHT). Red indicates high levels of
943 expression, blue indicates low levels of expression, and grey indicates no reads detected.
944 Hierarchical clustering is shown at top

945

946

947

948

949

950

951

952

953

954

955 **Supplemental Figure 3**

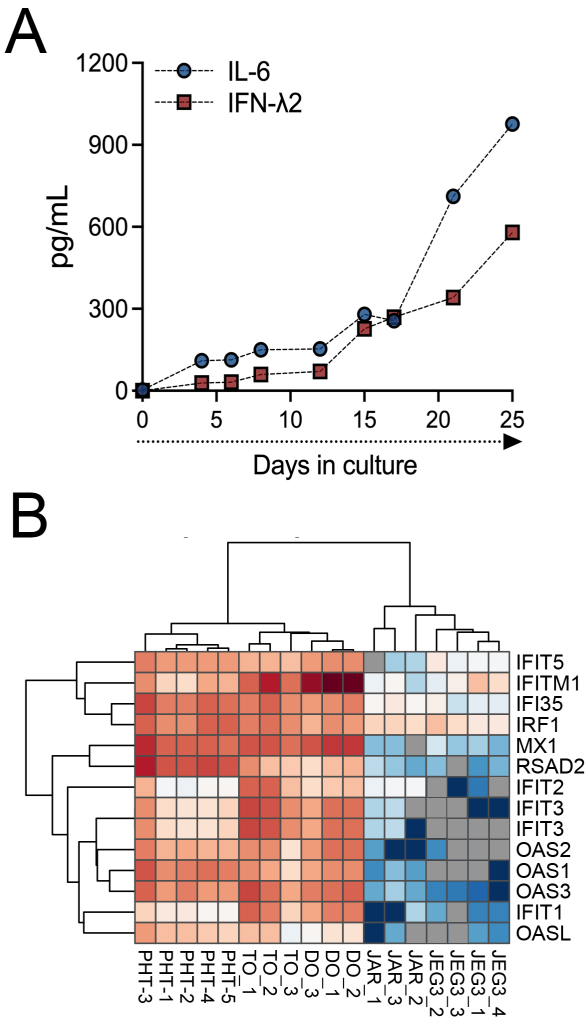

956

957 **Supplemental Figure 3. IFNs and ISGs in TOs and DOs. (A)** Concentrations of IL-6 (blue) and
958 IFN-λ2 (red) in CM generated from a single TO line throughout the first 25 days of culture. **(B)**
959 Heatmap (based on log2 RPKM values) of representative interferon stimulated genes (ISGs) in
960 TOs, DOs, primary human trophoblasts (PHT), or in JAR or JEG-3 cells. Red indicates high levels
961 of expression, blue indicates low levels of expression, and grey indicates no reads detected.
962 Hierarchical clustering is shown at top.
963

964

965

966

967

968 **Supplemental Figure 4**

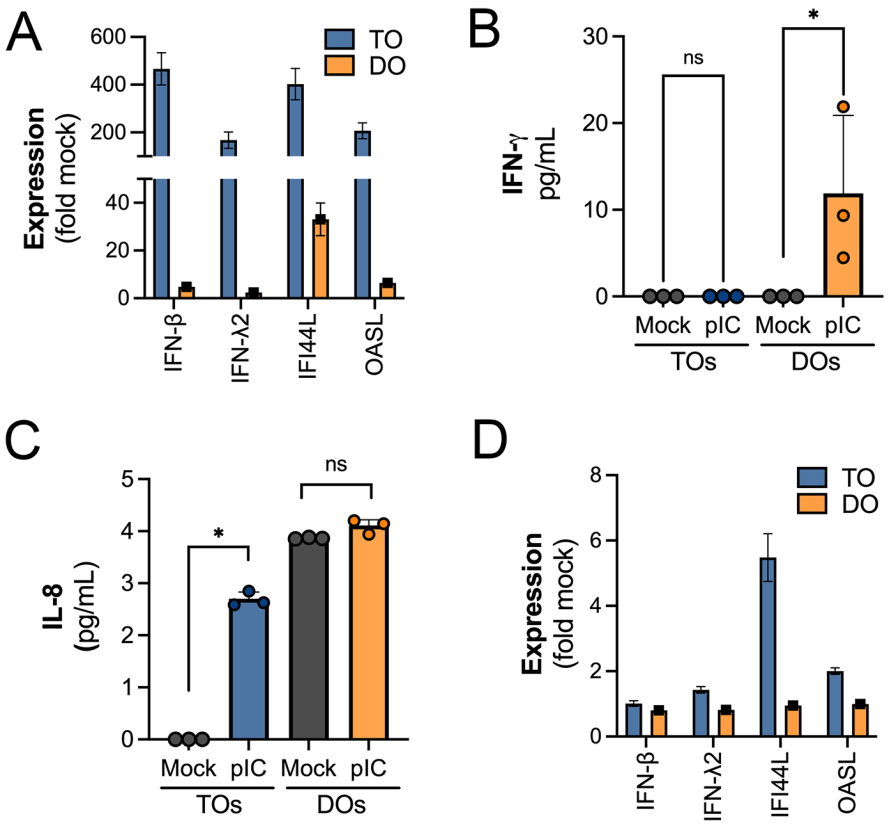

969

970 **Supplemental Figure 4. (A)** RT-qPCR for IFN-β, IFNλ-2, IFI44L, and OASL in poly I:C treated TOs
971 (blue) and DOs (orange). Data are shown as mean ± standard deviation as a fold change from mock-
972 treated controls. **(B, C)** Levels of IFN-γ (B) or IL-8 (C) as assessed by Luminex in TOs (blue) and
973 DOs (orange) treated with poly I:C or in mock-treated controls (grey). Data are shown as mean ±
974 standard deviation. Symbols represents unique organoid preparations. **(D)** RT-qPCR for IFN-β,
975 IFNλ-2, IFI44L, and OASL in ZIKV-infected TOs (blue) and DOs (orange) 72hrs post-infection. Data
976 are shown as mean ± standard deviation as a fold change from mock-infected controls. Significance
977 was determined with Mann-Whitney U test. *, $p<0.05$, ns, not significant.
978
979

980

981

982

983

984

985 **Table S1. qPCR primers used in this study.**

Target	Forward, 5'→3'	Reverse, 5'→3'
Actin	ACTGGGACGACATGGAGAAAAA	GCCACACGCAGCTC
IFN-β	GAGCTACAACTTGCTTGGATTC	CAAGCCTCCCATTCAATTGC
IFN-λ2	ACATAGCCCAGTTCAAGTC	GACTCTTCTAAGGCATCTTTG
IFI44L	AACCTAGACGACATAAAGAGG	CTGAAACCAAGTCTGCATAG
OASL	GTACCAGCAGTATGTGAAAG	ATGGTTAGAAGTTCAAGAGC
GATA3	AAAATGAACGGACAGAACC	GGGGTCTGTTAATATTGTGAAG
MUC20	CTCTTCCTTCTGTCCCTC	CCATTTTCACCTGCACTC
ZIKV	AGATGACTGCGTTGTGAAGC	GAGCAGAACGGGACTTCTTC

986

987

988